Table 1. IC_{50} of folate-linked liposomal doxorubicin with KB cells

Formulation	IC_{50} (μg/mL)
Free doxorubicin	0.65
NL	2.39
0.25F5-NL	1.15
SL	3.37
0.03F5-SL	2.70
0.25F5-SL	1.27
ML	1.62

NOTE: Mean (n = 5).

F-PEG-DSPE had the highest association rate, showing ~3-fold greater association than nontargeted liposomes (NL). Furthermore, we compared the uptake of NL and SL modified with F-PEG_{5000}-DSPE, with the NL form showing the highest uptake (Fig. 2B). The association of 0.25F5-SL was reduced in comparison with 0.25F5-NL. Therefore, we selected 0.25F5-SL and 0.25F5-NL and compared with ML.

To compare cellular uptake of three types of liposomes, stability was evaluated by drug release. 0.25F5-SL, 0.25F5-NL, and ML were not leaky because <2% drug release was observed over a 8 h incubation period at 37°C (Supplementary Fig. S2). This result indicates that the quantity of folate modification did not affect the stability of liposomal doxorubicin.

Cellular uptake of 0.25F5-SL, 0.25F5-NL, and ML was examined in FR(+) KB and FR(-) A549 cells by flow cytometry. Cellular association of doxorubicin to KB cells was higher ML < 0.25F5-SL < 0.25F5-NL irrespective of the same 0.25 mol% folate modification (Supplementary Fig. S3). Additionally, these increased associations of 0.25F5-SL and 0.25F5-NL to KB cells could be completely blocked by adding 1 mmol/L free folic acid to the medium, but those of ML was not changed. Lower association of 0.25F5-SL and 0.25F5-NL to A549 cells was observed compared with that to KB cells, but similar association of ML was observed to both cells. PEG layer may disturb interaction of folate with FR; therefore, ML may be effectively masked by folate ligand because of less uptake nevertheless low concentration of PEG coating than 0.25F5-SL.

To investigate difference of cellular uptake among 0.25F5-SL, 0.25F5-NL, and ML, the intracellular localization of the liposomes was observed by confocal laser scanning microscopy. Fluorescence images of KB and A549 cells after incubation with liposomes for 1 h are shown in Supplementary Fig. S4. Doxorubicin fluorescence was detected as red color within cells. Higher cellular uptake of 0.25F5-SL and 0.25F5-NL to KB cells was observed than that to A549 cells, whereas ML was not taken up to both cells. This indicated that, similar to result from cellular uptake by flow cytometry, ML was masked efficiently to KB cells.

Effect of F-PEG-DSPE in folate-linked liposomal doxorubicin on cytotoxicity. To confirm the optimal density and PEG spacer length of F-PEG-DSPE in liposomes, the cytotoxicity with KB cells was measured using a WST-8 assay. Doxorubicin concentrations leading to 50% cell death (IC_{50}) were determined from the concentration-dependent cell viability curves. As shown in Table 1, the IC_{50} value of 0.25F5-NL was the highest at 1.15 μg/mL. PEGylated liposomal doxorubicin, SL (IC_{50}, 3.37 μg/mL), showed lower toxicity than NL (IC_{50}, 2.39 μg/mL). However, modification of PEGylated liposomes by 0.25 mol% folate (0.25F5-SL) showed ~2.7 times higher toxicity (IC_{50}, 1.27 μg/mL) than SL, giving a similar level of cytotoxicity to folate-linked liposomes (0.25F5-NL). Free doxorubicin (IC_{50}, 0.65 μg/mL) showed much higher cytotoxicity than the liposomes. However, because free doxorubicin has a rapid systemic clearance rate, liposomes, especially with FR targeting, are likely to exhibit a therapeutic advantage over free doxorubicin *in vivo*.

The cellular uptake of folate-linked liposomes was increased by a longer PEG spacer and a higher density of F-PEG-DSPE. Such an increment corresponded well with enhanced cytotoxicity. Cellular association of SL was decreased because the mPEG layers inhibited interaction with cells, resulting in a cytotoxicity reduction. The major benefits of the mPEG layer exist only *in vivo*.

These results concerning folate-PEG spacer length in both NL and SL corresponded well with the previous report evaluated by cellular binding *in vitro*, in which the conjugation of folate to a shorter PEG spacer reduced folate exposure by interference with the ability of the liposome to recognize FR (8). With regard to folate density, maximal FR-dependent uptake of both NL and SL was obtained previously with a density of 0.2 to 0.5 mol% F-PEG-DSPE (10, 17, 28, 29). Our data on cellular uptake and *in vitro* cytotoxicity indicated that 0.25 mol% F5-PEG-DSPE in liposomes was optimal for targeting to FR on KB cells. It is known that the folate molecule can form dimers, trimers, and even self-assembling tubular quartets at higher concentrations (18). Similar to other glycosyl phosphatidylinositol-anchored proteins, FR molecules exist as clusters in specialized microdomains in the plasma membrane. Because FR can only bind one molecule of folic acid (19), such self-assembled multimers of folic acid are incapable of binding to FR. Therefore, an increase in the density of folate ligand on liposomes may not increase the level of binding to FR. The targeting efficiency of folate-linked vesicles was affected by the amount of folate-PEG lipid.

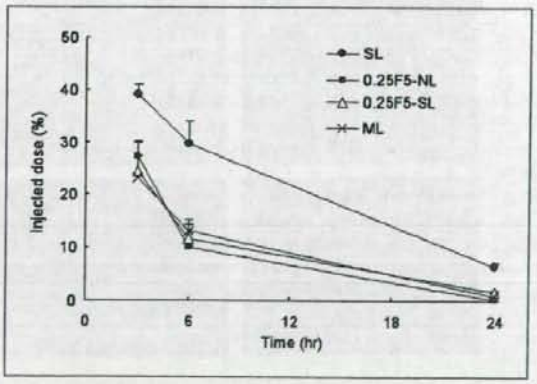

Fig. 3. Plasma concentration versus time curves of liposomal doxorubicin in mice. Liposomes were administered intravenous via tail vein injection at a dose of 5 mg/kg doxorubicin. The formulations used were SL (●), 0.25F5-SL (△), 0.25F5-NL (■), and ML (×). Mean ± SD (n = 3).

Table 2. Pharmacokinetic variables of liposomal doxorubicin in mice

Liposome	$AUC_{0\text{-}24\ h}$ (μg · h/mL)	Clearance (mL/h)
SL	491.2 ± 33.9**	0.3 ± 0.02
0.25F5-NL	190.2 ± 24.2**	0.7 ± 0.1
0.25F5-SL	212.1 ± 33.2**	0.6 ± 0.1
ML	218.0 ± 18.4**	0.6 ± 0.1

**, $P < 0.01$.

Serum doxorubicin level in mice after intravenous injection of folate-linked liposomal doxorubicin formulations. ML was designed to achieve a longer circulation time in the blood and also FR recognition on the tumor surface. The serum clearance kinetics of the various liposomal formulations in mice was compared as shown in Fig. 3 and Table 2. SL (AUC = 491.2 μg h/mL) exhibited a significantly longer circulation time than ML (AUC = 218.0 μg h/mL; clearance = 0.6 mL/h), 0.25F5-SL (AUC = 212.1 μg h/mL; clearance = 0.6 mL/h), and 0.25F5-NL (AUC = 190.2 μg h/mL; clearance = 0.7 mL/h; $P < 0.01$). Masking of the folate-linked liposomes, ML, did not achieve longer circulation times in the blood as well as 0.25F5-NL and 0.25F5-SL, as expected from the lower cellular uptake to KB cells. Our finding that 0.25F5-SL exhibited faster clearance than SL, corresponding with the previous study, indicated that the increase in folate modification of SL induced faster clearance than SL alone (9). This previous report indicated that this result was due to the distribution of folate-linked PEGylated liposomes over the internal organs, such as the liver, by the modification of folic acid (9). However, folate modification either inside or outside the mPEG-layer on the liposomes might lead to accumulation of liposomes in the tumor by FR targeting more significantly than the effect of longer circulation time. Next, we examined the distribution of folate-linked liposomal doxorubicin in tumors.

Distribution of folate-linked liposomal doxorubicin in M109 solid tumors. To evaluate the distribution of doxorubicin in

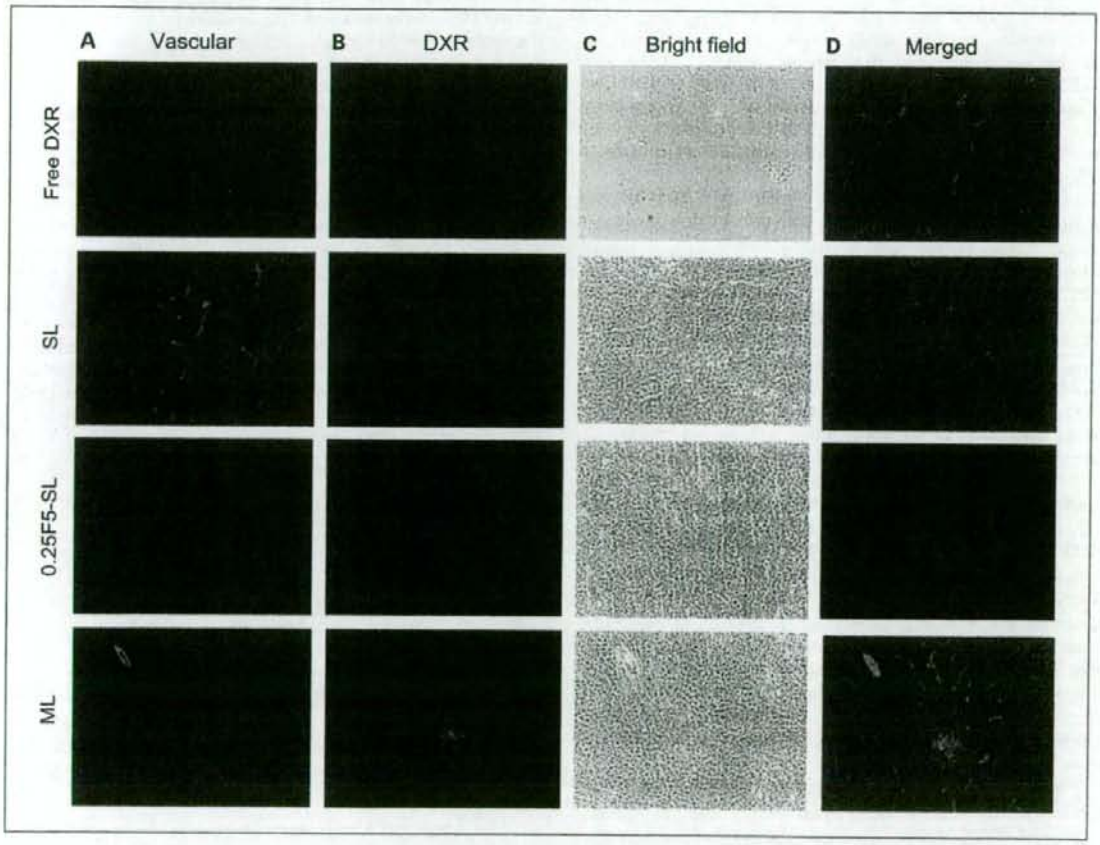

Fig. 4. Distribution of liposomal doxorubicin in M109 solid tumors measured by fluorescence microscopy. M109 cells were inoculated subcutaneously into female CDF1 mice. Twenty-four hours after intravenous administration of liposomes at a dose of 5 mg/kg doxorubicin, the tumor was excised and processed by frozen sectioning at 10 μm. Immunofluorescent staining of tumors by CD31 antibody is shown. Magnification, ×100. *Green signals*, location of neovessels; *red signals*, location of doxorubicin.

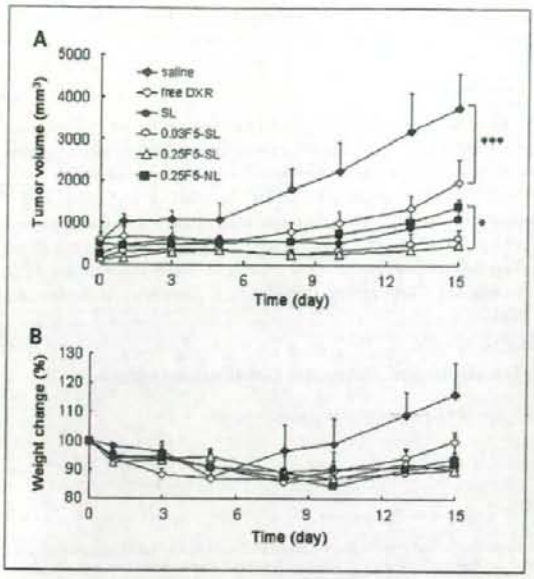

Fig. 5. Tumor growth inhibition by folate-linked liposomal doxorubicin in mice bearing M109 tumors. Tumor volume (*A*) and body weight change (*B*) after a single intravenous injection of liposomes at a dose of 10 mg/kg doxorubicin or with saline (♦). The formulations used were free doxorubicin (◇), SL (●), 0.03 F5-SL (○), 0.25F5-SL (△), and 0.25F5-NL (■). ***, $P < 0.001$; *, $P < 0.05$. Mean ± SD ($n = 6$).

tumors after intravenous injection of liposome formulations, we observed the staining of neovessels with FITC-fluorescent CD31 antibodies using a fluorescence microscope (Fig. 4). Most of the red fluorescence due to free doxorubicin was not observed in tumors 24 h later, but doxorubicin was observed in other liposome formulations. Folate-linked liposomes, ML, tended to accumulate around blood vessels, although a big difference was not seen in comparison with SL and 0.25F5-SL. This finding indicated that folate-linked liposomal doxorubicin accumulated in the tumor, whereas it did not show long circulation as SL.

Antitumor effect of folate-linked liposomal doxorubicin evaluated in M109 solid tumors. Because the folate-linked liposomes of 0.25F5-NL and 0.25F5-SL showed higher cytotoxicity than nontargeted PEGylated liposomes (SL) *in vitro*, their antitumor effect was evaluated in mice bearing M109 cells, including 0.03F5-SL and ML. At first, each preparation of liposomes (SL, 0.03F5-SL, 0.25F5-SL, and 0.25F5-NL) and free doxorubicin solution were injected intravenously at doses of 10 mg/kg doxorubicin body weight.

As shown in Fig. 5A, the doxorubicin-injected group showed a high antitumor effect in comparison with saline-treated and free doxorubicin-treated groups. The antitumor effect of folate-linked PEGylated liposomes, 0.25F5-SL, was significantly higher than that of folate-linked non-PEGylated liposomes, 0.25F5-NL, on day 15 ($P < 0.05$).

Next as shown in Fig. 6A, the antitumor effect of free doxorubicin, 0.25F5-SL, 0.25F5-NL, and SL was compared with that of ML after intravenous injection at doses of 8 mg/kg doxorubicin body weight. ML showed similar effect with 0.25F5-SL, and both liposomes showed a significantly higher antitumor effect compared with 0.25F5-NL and free doxorubicin ($P < 0.01$) but not with SL ($P > 0.05$) on day 16. SL showed a significantly higher effect with 0.25F5-NL ($P < 0.05$).

Moreover, as a result of observation of side effects by administering doxorubicin, a tendency of weight loss was seen shortly after administering free doxorubicin but not for liposomal doxorubicin (Figs. 5 and 6B). In addition, conspicuous side effects such as diarrhea were not observed with liposomal doxorubicin.

The antitumor effect of folate-linked liposomal doxorubicin, ML, and 0.25F5-SL was not significantly higher than that of SL, which was not related to the accumulation of doxorubicin in blood vessels in the tumor region (as shown in Fig. 4). This phenomenon might be ascribed to the difference in drug release rate, which is regarded as an important factor influencing the biological activity of liposomal drugs (30, 31). In order for folate-linked liposomes to bind FR in a solid tumor via intravenous injection, they require extravasation from blood vessels in the tumor region, passage through the intercellular space, and finally reach FR on the tumor cell surface. Although folate-linked liposomal doxorubicin was retained in the tumor, release of the drug into the local environment might vary. After accumulation in the tumor, SL could effectively release the encapsulated drug and free

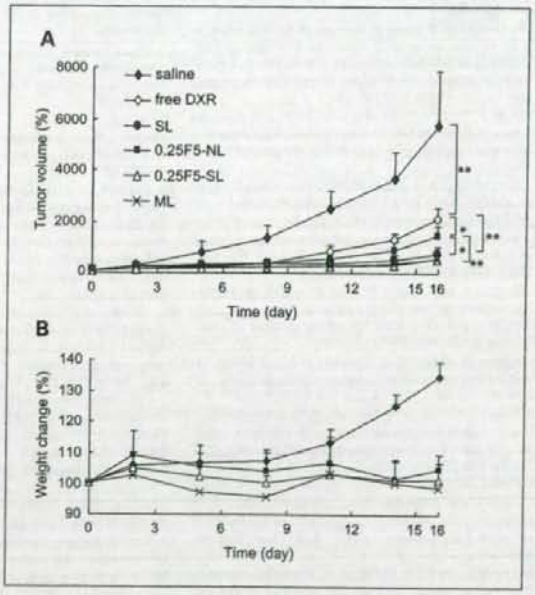

Fig. 6. Tumor growth inhibition by folate-linked and masked folate-linked liposomal doxorubicin in mice bearing M109 tumors. Tumor volume (*A*) and body weight change (*B*) after a single intravenous injection of liposomes at a dose of 8 mg/kg doxorubicin or with saline (♦). The formulations used were free doxorubicin (◇), SL (●), 0.25F5-SL (△), 0.25F5-NL (■), and ML (×). Tumor volumes are plotted as ratios to their volume before the first drug injection. Mean ± SD ($n = 6$) **, $P < 0.01$; *, $P < 0.05$.

doxorubicin rapidly reached a therapeutic concentration that can inhibit tumor growth. In contrast, ML and 0.25F5-SL could accumulate relatively highly in the tumor but could not release the required amount of drug at an appropriate rate. In a nonsolid tumor, the high therapeutic efficacy of folate-linked liposomal doxorubicin was reported in mouse ascites leukemia models, in which the treatment route was intraperitoneal injection (14). In addition, the therapeutic efficacy of intravenous treatment with folate-linked liposomal doxorubicin was improved in mice inoculated intraperitoneally with lymphoma cells (32, 33). Therefore, further study is needed for FR targeting of solid tumors by intravenous injection of folate-linked liposomes. These findings suggested that, for active targeting using folate following intravenous injection, the sterically stabilized property of liposomes was needed as well as targeting to retard tumor growth, in contrast to the *in vitro* results. Folate-linked SLs and MLs with less circulation times showed comparative antitumor effect to traditional SL. Longer linker of folate and less PEG modification will allow the design of FR targeting liposome in the clinical setting.

Conclusion

In this study, the effects of PEG spacer length and ligand density on FR-targeted liposomes were evaluated. Folate ligands with 0.25 mol% and sufficiently long PEG spacers (F-PEG_{5000}-DSPE) of NLs increased the FR association and cytotoxicity compared with those of SLs and MLs *in vitro*. On the contrary, folate-linked SLs and MLs showed a higher tumor-killing effect than folate-linked NLs *in vivo*. Further study to optimize PEG coating for FR-targeting particles will improve the antitumor effect.

Disclosure of Potential Conflicts of Interest

No potential conflicts of interest were disclosed.

References

1. Weitman SD, Lark RH, Coney LR, et al. Distribution of the folate receptor GP38 in normal and malignant cell lines and tissue. Cancer Res 1992;52:3396–401.
2. Wu M, Gunning W, Ratnam M. Expression of folate receptor type α in relation to cell type, malignancy, and differentiation in ovary, uterus, and cervix. Cancer Epidemiol Biomarkers Prev 1999;8:775–82.
3. Elnakat H, Ratnam M. Distribution, functionality and gene regulation of folate receptor isoforms: implications in targeted therapy. Adv Drug Deliv Rev 2004; 56:1067–84.
4. Shen F, Ross JF, Wang X, Ratnam M. Identification of a novel folate receptor, a truncated receptor, and receptor type β in hematopoietic cells: cDNA cloning, expression, immunoreactivity, and tissue specificity. Biochemistry 1994;33:1209–15.
5. Ross JF, Wang H, Behm FG, et al. M. Folate receptor type β is a neutrophilic lineage marker and is differentially expressed in myeloid leukemia. Cancer 1999;85: 348–57.
6. Wang H, Ross JF, Ratnam M. Structure and regulation of a polymorphic gene encoding folate receptor type γ/γ'. Nucleic Acids Res 1998;26:2132–42.
7. Lee RJ, Low PS. Folate-mediated tumor cell targeting of liposome entrapped doxorubicin *in vitro*. Biochim Biophys Acta 1995;1233:134–44.
8. Gabizon A, Horowitz AT, Goren D, et al. Targeting folate receptor with folate linked to extremities of poly (ethylene glycol)-grafted liposomes: *in vitro* studies. Bioconjug Chem 1999;10:289–98.
9. Gabizon A, Horowitz AT, Goren D, et al. *In vivo* fate of folate-targeting polyethylene-glycol liposomes in tumor-bearing mice. Clin Cancer Res 2003;9:6551–9.
10. Goren D, Horowitz AT, Tzemach D, et al. Nuclear delivery of doxorubicin via folate-targeted liposomes with bypass of multidrug-resistance efflux pump. Clin Cancer Res 2000;6:1949–57.
11. Sudimack J, Lee RJ. Drug targeting via the folate receptor. Adv Drug Deliv Rev 2000;41:147–62.
12. Hofland HE, Masson C, Iginla S, et al. Folate-targeted gene transfer *in vivo*. Mol Ther 2002;5: 739–44.
13. Pan XQ, Zheng X, Shi G, et al. A strategy for the treatment of acute myelogenous leukemia based on folate receptor type-targeted liposomal doxorubicin combined with receptor induction using all-*trans*-retinoic acid. Blood 2002;100:594–602.
14. Pan XQ, Wang H, Lee RJ. Antitumor activity of folate receptor-targeted liposomal doxorubicin in a KB oral carcinoma murine xenograft model. Pharm Res 2003; 20:417–22.
15. Rait AS, Pirollo KF, Xiang L, Ulick D, Chang EH. Tumor-targeting, systemically delivered antisense HER-2 chemosensitizes human breast cancer xenografts irrespective of HER-2 levels. Mol Med 2002; 8:475–86.
16. Zhao X, Lee RJ. Tumor-selective targeted delivery of genes and antisense oligodeoxyribonucleotides via the folate receptor. Adv Drug Deliv Rev 2004;56: 1193–204.
17. Reddy JA, Abburi C, Hofland H, et al. Folate-targeted, cationic liposome-mediated gene transfer into disseminated peritoneal tumors. Gene Ther 2002;9: 1542–50.
18. Ciuchi F, Di Nicola G, Franz H, et al. Self-recognition and self-assembly of folic acid salts: columnar liquid crystalline polymorphism and the column growth process. J Am Chem Soc 1994;116:7064–71.
19. Antony AC, Utley C, Van Horne KC, Kolhouse JF. Isolation and characterization of a folate receptor from human placenta. J Biol Chem 1981;256:9684–92.
20. Shiokawa T, Hattori Y, Kawano K, et al. Effect of polyethylene glycol linker spacer length of folate-linked microemulsions loading aclacinomycin A on targeting ability and antitumor effect *in vitro* and *in vivo*. Clin Cancer Res 2005;11:2018–25.
21. Hayama A, Yamamoto T, Yokoyama M, et al. Polymeric micelles modified by folate-PEG-lipid for targeted drug delivery to cancer cells *in vitro*. J Nanosci Nanotech 2008;8:1–8.
22. Uster PS, Allen TM, Daniel BE, et al. Insertion of poly(ethylene glycol) derivatized phospholipid into pre-formed liposomes results in prolonged *in vivo* circulation time. FEBS Lett 1996;386:243–46.
23. Lee RJ, Wang S, Turk MJ, Low PS. The effects of pH and intraliposomal buffer strength on the rate of liposome content release and intracellular drug delivery. Biosci Rep 1998;18:69–78.
24. Matsushita Y, Iguchi H, Kiyosaki T, et al. A high performance liquid chromatographic method of analysis of 4'-*O*-tetrahydropyranyladriamycin and their metabolites in biological samples. J Antibiot (Tokyo) 1983; 36:880–6.
25. Takemoto S, Yamaoka K, Nishikawa M, Takakura Y. Histogram analysis of pharmacokinetic parameters by bootstrap resampling from one-point sampling data in animal experiments. Drug Metab Pharmacokinet 2006;21:458–64.
26. Li X, Hirsh DJ, Cabral-Lilly D, et al. Doxorubicin physical state in solution and inside liposomes loaded via a pH gradient. Biochim Biophys Acta 1998;1415: 23–40.
27. Paulos CM, Reddy JA, Leamon CP, et al. Ligand binding and kinetics of folate receptor recycling *in vivo*: impact on receptor-mediated drug delivery. Mol Pharmacol 2004;66:1406–14.
28. Saul JM, Annapragada A, Natarajan JV, Bellamkonda RV. Controlled targeting of liposomal doxorubicin via the folate receptor *in vitro*. J Control Release 2003;92:49–67.
29. Shmeeda H, Mak L, Tzemach D, et al. Intracellular uptake and intracavitary targeting of folate-conjugated liposomes in a mouse lymphoma model with up-regulated folate receptors. Mol Cancer Ther 2006;5: 818–24.
30. Cui J, Li C, Guo W, et al. Direct comparison of two pegylated liposomal doxorubicin formulations: is AUC predictive for toxicity and efficacy? J Control Release 2007;118:204–15.
31. Lim HJ, Masin D, Madden TD, Bally MB. Influence of drug release characteristics on the therapeutic activity of liposomal mitoxantrone. J Pharmacol Exp Ther 1997;281:566–73.
32. Gabizon A, Shmeeda H, Horowitz AT, Zalipsky S. Tumor cell targeting of liposome-entrapped drugs with phospholipid-anchored folic acid-PEG conjugates. Adv Drug Deliv Rev 2004;56:1177–92.
33. Shmeeda H, Mak L, Tzemach D, Astrahan P, Tarshish M, Gabizon A. Intracellular uptake and intracavitary targeting of folate-conjugated liposomes in a mouse lymphoma model with up-regulated folate receptors. Mol Cancer Ther 2006;5:818–24.

Int. J. Cancer: **122**, 2148–2153 (2008)

Synergistic antitumor activity of the novel SN-38-incorporating polymeric micelles, NK012, combined with 5-fluorouracil in a mouse model of colorectal cancer, as compared with that of irinotecan plus 5-fluorouracil

Takako Eguchi Nakajima[1,2], Masahiro Yasunaga[2], Yasuhiko Kano[3], Fumiaki Koizumi[4], Ken Kato[1], Tetsuya Hamaguchi[1], Yasuhide Yamada[1], Kuniaki Shirao[1], Yasuhiro Shimada[1] and Yasuhiro Matsumura[2]*

[1]*Gastrointestinal Oncology Division, National Cancer Center Hospital, Tokyo, Japan*
[2]*Investigative Treatment Division, Research Center for Innovative Oncology, National Cancer Center Hospital East, Kashiwa, Chiba, Japan*
[3]*Hematology Oncology, Tochigi Cancer Center, Tochigi, Japan*
[4]*Shien Lab Medical Oncology Division, National Cancer Center Hospital, Tokyo, Japan*

The authors reported in a previous study that NK012, a 7-ethyl-10-hydroxy-camptothecin (SN-38)-releasing nano-system, exhibited high antitumor activity against human colorectal cancer xenografts. This study was conducted to investigate the advantages of NK012 over irinotecan hydrochloride (CPT-11) administered in combination with 5-fluorouracil (5FU). The cytotoxic effects of NK012 or SN-38 (an active metabolite of CPT-11) administered in combination with 5FU was evaluated *in vitro* in the human colorectal cancer cell line HT-29 by the combination index method. The effects of the same drug combinations was also evaluated *in vivo* using mice bearing HT-29 and HCT-116 cells. All the drugs were administered i.v. 3 times a week; NK012 (10 mg/kg) or CPT11 (50 mg/kg) was given 24 hr before 5FU (50 mg/kg). Cell cycle analysis in the HT-29 tumors administered NK012 or CPT-11 *in vivo* was performed by flow cytometry. NK012 exerted more synergistic activity with 5FU compared to SN-38. The therapeutic effect of NK012/5FU was significantly superior to that of CPT-11/5FU against HT-29 tumors ($p = 0.0004$), whereas no significant difference in the antitumor effect against HCT-116 tumors was observed between the 2-drug combinations ($p = 0.2230$). Cell-cycle analysis showed that both NK012 and CPT-11 tend to cause accumulation of cells in the S phase, although this effect was more pronounced and maintained for a more prolonged period with NK012 than with CPT-11. Optimal therapeutic synergy was observed between NK012 and 5FU, therefore, this regimen is considered to hold promise of clinical benefit, especially for patients with colorectal cancer.
© *2008 Wiley-Liss, Inc.*

Key words: NK012; SN-38; 5-fluorouracil; drug delivery system; colorectal cancer

The 5-year survival rates of colorectal cancer (CRC) have improved remarkably over the last 10 years, accounted for in large part by the extensively investigated agents after 5-fluorouracil (5FU). Irinoetcan hydrochloride (CPT-11), a water-soluble, semi-synthetic derivative of camptothecin, is one such agent that has been shown to be highly effective, and currently represents a key-drug in first- and second-line treatment regimens for CRC. CPT-11 monotherapy, however, has not been shown to yield superior efficacy, including in terms of the median survival time, to bolus 5FU/leucovorin (LV) alone.[1] In 2 Phase III trials, the addition of CPT-11 to bolus or infusional 5FU/LV regimens clearly yielded greater efficacy than administration of 5FU/LV alone, with a doubling of the tumor response rate and prolongation of the median survival time by 2–3 months.[1,2]

CPT-11 is converted to 7-ethyl-10-hydroxy-camptothecin (SN-38), a biologically active and water-insoluble metabolite of CPT-11, by carboxylesterases in the liver and the tumor. SN-38 has been demonstrated to exhibit up to a 1,000-fold more potent cytotoxic activity than CPT-11 against various cancer cells *in vitro*.[3] The metabolic conversion rate is, however, very low, with only <10% of the original volume of CPT-11 being metabolized to SN-38[4,5]; conversion of CPT-11 to SN-38 also depends on genetic interindividual variability of the activity of carboxylesterases.[6] Direct use of SN-38 itself for clinical cancer treatment must be shown to be identical in terms of both efficacy and toxicity.

Some drugs incorporated in drug delivery systems (DDS), such as Abraxane and Doxil, are already in clinical use.[7,8] The clinical benefits of DDS are based on their EPR effect.[9] The EPR effect is based on the pathophysiological characteristics of solid tumor tissues: hypervascularity, incomplete vascular architecture, secretion of vascular permeability factors stimulating extravasation within cancer tissue, and absence of effective lymphatic drainage from the tumors that impedes the efficient clearance of macromolecules accumulated in solid tumor tissues. Several types of DDS can be used for incorporation of a drug. A liposome-based formulation of SN-38 (LE-SN38) has been developed, and a clinical trial to assess its efficacy is now under way.[10,11]

Recently, we demonstrated that NK012, novel SN-38-incorporating polymeric micelles, exerted superior antitumor activity and less toxicity than CPT-11.[12] NK012 is characterized by a smaller size of the particles than LE-SN38; the mean particle diameter of NK012 is 20 nm. NK012 can release SN-38 under neutral conditions even in the absence of a hydrolytic enzyme, because the bond between SN-38 and the block copolymer is a phenol ester bond, which is stable under acidic conditions and labile under mild alkaline conditions. The release rate of SN-38 from NK012 under physiological conditions is quite high; more than 70% of SN-38 is released within 48 hr. We speculated that the use of NK012, in place of CPT-11, in combination with 5FU may yield superior results in the treatment of CRC. In the present study, we evaluated the antitumor activity of NK012 administered in combination with 5FU as compared to that of CPT-11 administered in combination with 5FU against CRC in an experimental model.

Material and methods

Cells and animals

The human colorectal cancer cell lines used, namely, HT-29 and HCT-116, were purchased from the American Type Culture Collection (Rockville, MD). The HT-29 cells and HCT-116 cells were maintained in RPMI 1640 supplemented with 10% fetal bovine serum (Cell Culture Technologies, Gaggenau-Hoerden, Germany), penicillin, streptomycin, and amphotericin B (100 units/mL, 100 μg/mL, and 25 μg/mL, respectively; Sigma, St. Louis, MO) in a humidified atmosphere containing 5% CO_2 at 37°C.

BALB/c *nu/nu* mice were purchased from SLC Japan (Shizuoka, Japan). Six-week-old mice were subcutaneously (s.c.)

*Correspondence to: Investigative Treatment Division, Research Center for Innovative Oncology, National Cancer Center Hospital East, 6-5-1 Kashiwanoha, Kashiwa, Chiba 277-8577, Japan. Fax: +81-4-7134-6866. E-mail: yhmatsum@east.ncc.go.jp
Received 2 September 2007; Accepted after revision 20 November 2007
DOI 10.1002/ijc.23381
Published online 14 January 2008 in Wiley InterScience (www.interscience.wiley.com).

inoculated with 1×10^6 cells of HT-29 or HCT-116 cell line in the flank region. The length (a) and width (b) of the tumor masses were measured twice a week, and the tumor volume (TV) was calculated as follows: $TV = (a \times b^2)/2$. All animal procedures were performed in compliance with the Guidelines for the Care and Use of Experimental Animals established by the Committee for Animal Experimentation of the National Cancer Center; these guidelines meet the ethical standards required by law and also comply with the guidelines for the use of experimental animals in Japan.

Drugs

The SN-38-incorporating polymeric micelles, NK012, and SN-38 were prepared by Nippon Kayaku (Tokyo, Japan).[12] CPT-11 was purchased from Yakult Honsha (Tokyo, Japan). 5FU was purchased from Kyowa Hakko (Tokyo, Japan).

Cell growth inhibition assay

HT-29 cells were seeded in 96-well plates at a density of 2,000 cells/well in a final volume of 90 μL. Twenty-four hours after seeding, a graded concentration of NK012 or SN-38 was added concurrently with 5FU to the culture medium of the HT-29 cells in a final volume of 100 μL for drug interaction studies. The culture was maintained in the CO_2 incubator for an additional 72 hr. Then, cell growth inhibition was measured by the tetrazolium salt-based proliferation assay (WST assay; Wako Chemicals, Osaka, Japan). WST-1 labeling solution (10 μL) was added to each well and the plates were incubated at 37°C for 3 hr. The absorbance of the formazan product formed was detected at 450 nm in a 96-well spectrophotometric plate reader. Cell viability was measured and compared to that of the control cells. Each experiment was carried out in triplicate and was repeated at least 3 times. Data were averaged and normalized against the nontreated controls to generate dose-response curves.

Drug interaction analysis

The nature of interaction between NK012 or SN-38 and 5FU against HT-29 cells was evaluated by median-effect plot analyses and the combination index (CI) method of Chou and Talalay.[13] Data analysis was performed using the Calcusyn software (Biosoft, NY, USA). NK012 or SN-38 was combined with 5FU at a fixed ratio that spanned the individual IC_{50} values of each drug. The IC_{50} values were determined on the basis of the dose-response curves using the WST assay. For any given drug combination, the CI is known to represent the degree of synergy, additivity or antagonism. It is expressed in terms of fraction-affected (Fa) values, which represents the percentage of cells killed or inhibited by the drug. Isobologram equations and Fa/CI plots were constructed by computer analysis of the data generated from the median effect analysis. Each experiment was performed in triplicate with 6 gradations and was repeated at least 3 times. The resultant dose-response curves were averaged, to create a single composite dose-response curve for each combination.

In vivo analysis of the effects of NK012 combined with 5FU as compared to those of CPT-11 combined with 5FU

When the mean tumor volumes reached ~93 mm^3, the mice were randomly divided into test groups consisting of 5 mice per group (Day 0). The drugs were administered i.v. *via* the tail vein of the mice. In the groups administered NK012 or 5FU as single agents, the drug was administered on Days 0, 7 and 14. In the combined treatment groups, NK012 or CPT-11 was administered 24 hr before 5FU on Days 0, 7 and 14, according to the previously reported combination schedule for CPT-11 and 5FU.[14] Complete response (CR) was defined as tumor not detectable by palpation at 90 days after the start of treatment, at which time-point the mice were sacrificed. Tumor volume and body weight were measured twice a week. As a general rule, animals in which the tumor volume exceeded 2,000 mm^3 were also sacrificed.

Experiment 1. Evaluation of the effects of NK012 combined with 5FU and determination of the maximum tolerated dose (MTD) of NK012/5FU. By comparing the data between NK012 administered as a single agent and NK012/5FU, we evaluated the effects of the combined regimen against the s.c HT-29 tumors. A preliminary experiment showed that combined administration of NK012 15 mg/kg + 5FU 50 mg/kg every 6 days caused drug-related lethality (data not shown). To determine the MTD, therefore, we set the dosing schedule of the combined regimen at 5 or 10 mg/kg of NK012 + 50 mg/kg of 5FU three times a week.

Experiment 2. Comparison of the antitumor effect of NK012/5FU and CPT-11/5FU. Based on a comparison of the data between NK012/5FU and CPT-11/5FU against the s.c. HT-29 and HCT-116 tumors, we investigated the feasibility of the clinical application of NK012/5FU for the treatment of CRC. CPT-11/5FU was administered three times a week at the respective MTDs of the 2 drugs as previously reported, that is, CPT11 at 50 mg/kg and 5FU at 50 mg/kg, respectively.[14] NK012/5FU was administered once three times a week at the respective MTDs of the 2 drugs determined from Experiment 1.

Cell cycle analysis

Samples from the HT-29 tumors that had grown to 80–100 mm^3 were removed from the mice at 6, 24, 48, 72 and 96 hr after the administration of NK012 alone at 10 mg/kg or CPT-11 alone at 50 mg/kg. The samples were excised, minced in PBS and fixed in 70% ethanol at −20°C for 48 hr. They were then digested with 0.04% pepsin (Sigma chemical Co., St Lous, MO) in 0.1 N HCL for 60 min at 37°C in a shaking bath to prepare single-nuclei suspensions. The nuclei were then centrifuged, washed twice with PBS and stained with 40 μg/mL of propidium iodide (Molecular Probes, OR) in the presence of 100 μg/mL RNase in 1 mL PBS for 30 min at 37°C. The stained nuclei were analyzed with B-D FACSCalibur (BD Biosciences, San Jose, CA), and the cell cycle distribution was analyzed using the Modfit program (Verity Software House Topsham, ME).

Statistical analyses

Data were expressed as mean ± SD. Data were analysed with Student's t test when the groups showed equal variances (F test), or Welch's test when they showed unequal variances (F test). $p < 0.05$ was regarded as statistically significant. All statistical tests were 2-sided.

Results

Antiproliferative effects of NK012 or SN-38 administered in combination with 5FU

Figure 1*a* shows the dose-response curves for NK012 alone, 5FU alone and a combination of the two. The IC_{50} levels of NK012 and 5FU against the HT-29 cells were 39 nM and 1 μM, respectively, and the IC_{50} level of SN-38 was 14 nM (data not shown). Based on these data, the molar ratio of NK012 or SN-38:5FU of 1:1,000 was used for the drug combination studies.

Figures 1*b* and 1*c* show the median-effect and the combination index plots. Combination indices (CIs) of <1.0 are indicative of synergistic interactions between 2 agents; additive interactions are indicated by CIs of 1.0, and antagonism by CIs of >1.0. Figure 1*c* shows the combination index for NK012 and 5FU, when 2 drugs are supposed to be mutually exclusive. Marked synergism was observed between Fa 0.2 and 0.6. Theoretically, the CI method is the most reliable around an Fa of 0.5, suggesting synergistic effects of the combination of NK012 and 5FU. This synergistic effect was more evident than that of SN-38/5FU (Fig. 1*d*).

In vivo *effect of combined NK012 and 5FU*

Experiment 1. Dose optimization and effect of combined NK012 and 5FU against HT-29 tumors. Comparison of the relative tumor volumes on Day 40 revealed significant differences between

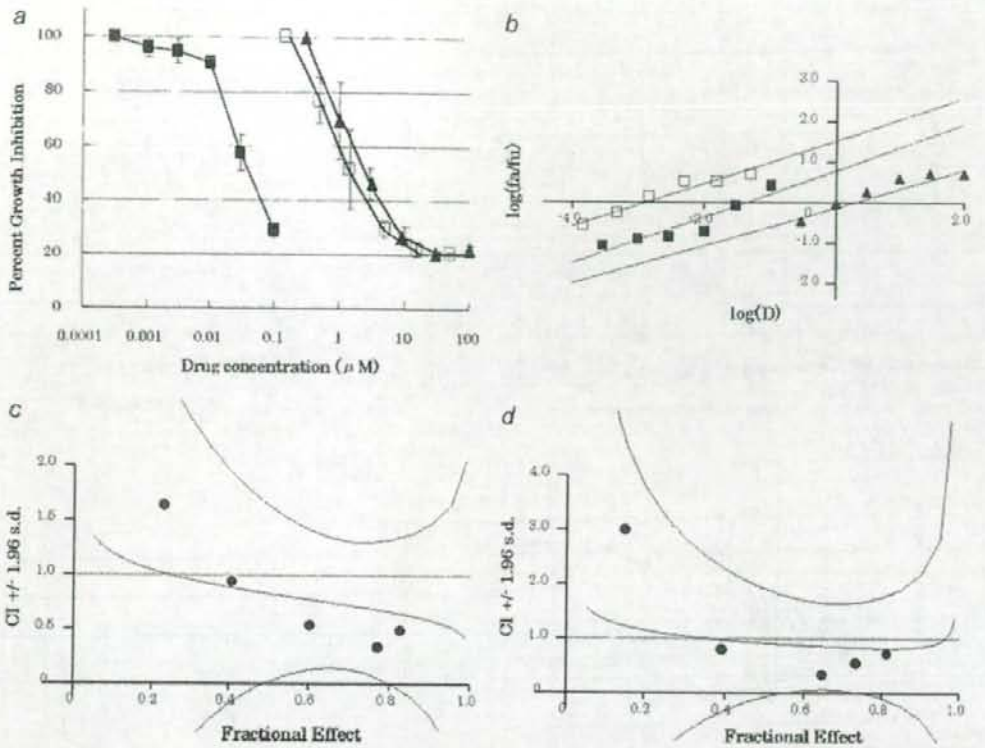

FIGURE 1 – Interaction of NK012 and 5FU *in vitro*. (*a*) Dose-response curves for NK012 alone (■), 5FU alone (▲) and their combination (□) against HT-29 cells. HT-29 cells were seeded at 2,000 cells/well. Twenty-four hours after seeding, a graded concentration of NK012 or 5FU was added to the culture medium of the HT-29 cells. Cell growth inhibition was measured by WST assay after 72 hr of treatment. Cell viability was measured and compared with that of the control cells. Each experiment was carried out independently and repeated at least 3 times. Points, mean of tripricates; bars, SD. (*b*) Median effect plot for the interaction of NK012 and 5FU. (*c, d*) Combination index for the interaction as a function of the level of effect (fraction effect = 0.5 is the IC_{50}). The straight line across the CI value of 1.0 indicates additive effect and CIs above and below indicate antagonism and synergism, respectively. The molar ratio of NK012/5FU (*c*) or SN-38/5FU (*d*) at 1:1,000 was tested by CI analysis. Black circles represent the CIs of the actual data points, solid lines represent the computer-derived CIs at effect levels ranging from 10 to 100% inhibition of cell growth, and the dotted lines represent the 95% confidence intervals.

those in the mice administered NK012 alone and those administered NK012/5FU at 5 mg/kg of NK012 ($p = 0.018$) (Fig. 2*a*). Although there was no statistically significant difference in the relative tumor volume measured on Day 54 between the mice administered NK012 alone and NK012/5FU at 10 mg/kg of NK012 ($p = 0.3050$), a trend of superior antitumor effect was demonstrated in the group treated with NK012/5FU at 10 mg/kg of NK012 (Fig. 2*a*). The CR rates were 20, 40 and 60% for 5 mg/kg NK012 + 50 mg/kg 5FU, 10 mg/kg NK012 alone and 10 mg/kg NK012 + 50 mg/kg 5FU, respectively. The schedule of 10 mg/kg NK012 + 50 mg/kg 5FU resulted in no remarkable toxicity in terms of body weight changes, and these doses were determined as representing the MTDs (Fig. 2*b*).

Experiment 2. Comparison of the antitumor effect of combined NK012/5FU and CPT-11/5FU against HT-29 and HCT-116 tumors. The therapeutic effect of NK012/5FU on Day 60 was significantly superior to that of CPT-11/5FU against the HT-29 tumors ($p = 0.0004$) (Fig. 3*a*). A more potent antitumor effect, namely, a 100% CR rate, was obtained in the NK012/5FU group as compared to the 0% CR rate in the CPT-11/5FU group. Although no statistically significant difference in the relative tumor volume on Day 61 was demonstrated between the NK012/5FU and CPT-11/5FU in the case of the HCT-116 tumors ($p = 0.2230$), a trend of superior antitumor effect against these tumors was observed in the NK012/5FU treatment group (Fig. 3*b*). The CR rates for the case of the HCT-116 tumors were 0% in both NK012/5FU and CPT-11/5FU groups.

Specificity of cell cycle perturbation

We studied the differences in the effects between NK012 10 mg/kg and CPT-11 50 mg/kg on the cell cycle (Fig. 4*a*). The data indicated that both NK012 and CPT-11 tended to cause accumulation of cells in the S phase, although the effect of NK012 was stronger and maintained for a more prolonged period than that of CPT-11; the maximal percentage of S-phase cells in the total cell population in the tumors was 34% at 24 hr after the administration of CPT-11, whereas it was 39% at 48 hr after the administration of NK012 (Figs. 4*b*, and 4*c*).

Discussion

Our primary endpoint was to clarify the advantages of NK012 over CPT-11 administered in combination with 5FU. We demonstrated that combined NK012 and 5FU chemotherapy exerts more

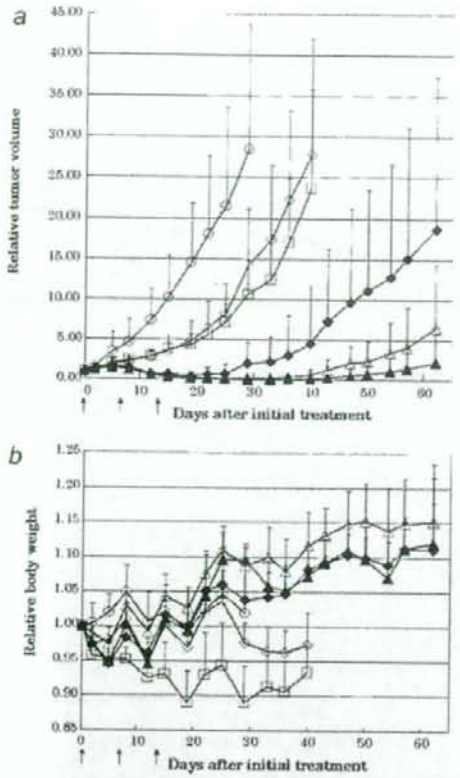

FIGURE 2 – Effect of NK012 alone or NK012 in combination with 5FU against HT-29 tumor-bearing mice. Points, mean; bars, SD. (*a*) Antitumor effect of each regimen on Days 0, 7 and 14. (○) control, (□) 5FU 50 mg/kg alone, (◇) NK012 5 mg/kg alone, (◆) NK012 5 mg/kg 24 hr before 5FU 50 mg/kg, (△) NK012 10 mg/kg alone, (▲) NK012 10 mg/kg 24 hr before 5FU 50 mg/kg. (*b*) Changes in the relative body weight. Data were derived from the same mice as those used in the present study.

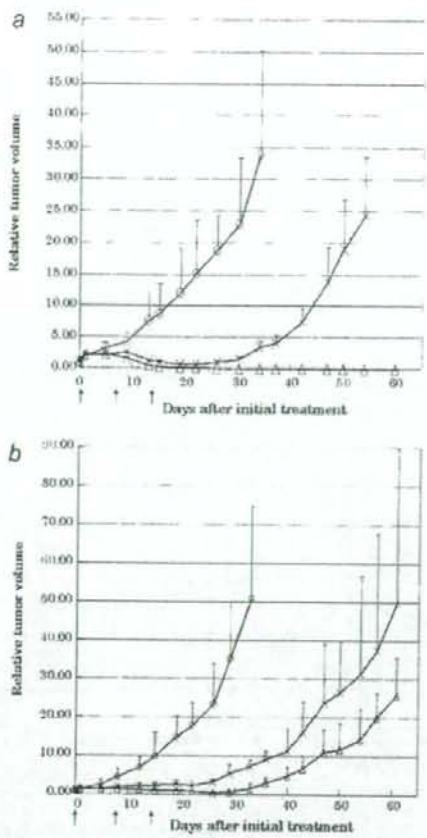

FIGURE 3 – Effect of NK012/5FU as compared with that of CPT11/5FU against HT-29 (*a*) or HCT-116 (*b*) tumor-bearing mice. Antitumor effect of each schedule on Days 0, 7 and 14. (○) control, (×) CPT-11 50 mg/kg 24 hr before 5FU 50 mg/kg, (△) NK012 10 mg/kg 24 hr before 5FU 50 mg/kg. Points, mean; bars, SD.

synergistic activity *in vitro* and significantly greater antitumor activity against human CRC xenografts as compared to CPT-11/5FU. The combination of NK012 and 5FU is considered to hold promise of clinical benefit for patients with CRC.

CPT-11, a topoisomerase-I inhibitor, and 5FU, a thymidilate synthase inhibitor, have been demonstrated to be effective agents for the treatment of CRC. A combination of these 2 drugs has also been demonstrated to be clearly more effective than either CPT-11 or 5FU/LV administered alone *in vivo* and in clinical settings.[1,2,14] Administration of 5FU by infusion with CPT-11 was shown to be associated with reduced toxicity and an apparent improvement in survival as compared to that of administration of the drug by bolus injection with CPT-11.[1,2] This synergistic enhancement may result from the mechanism of action of the 2 drugs; CPT-11 has been reported to cause accumulation of cells in the S phase, and 5FU infusion is known to cause DNA damage specifically in cells of the S phase.[14] On the basis of this background, our results suggesting the more pronounced and more prolonged accumulation of the tumor cells in the S phase caused by NK012 as compared with that by CPT-11 may explain the more effective synergy of the former administered with 5FU infusion. This may be attributable to accumulation of NK012 due to the enhanced permeability and retention (EPR) effect.[9] It is also speculated that NK012 allows sustained release of free SN-38, which may move more freely in the tumor interstitium.[15] Otherwise NK012 itself could internalize into cells to localize in several cytoplasmic organelles as reported by Savic *et al.*[16] These characteristics of NK012 may be responsible for its more potent antitumor activity observed in this study, because CPT-11 has been reported to show time-dependent growth-inhibitory activity against the tumor cells.[17]

The major dose-limiting toxicities of CPT-11 are diarrhea and neutropenia. SN-38, the active metabolite of CPT-11, may cause CPT-11-related diarrhea as a result of mitotic -inhibitory activity.[18] Because it undergoes significant biliary excretion, SN-38 may have a potentially long residence time in the gastrointestinal tract that may be associated with prolonged diarrhea.[19,20] In our previous report, we evaluated the tissue distribution of SN-38 after administration of an equimolar amount of NK012 (20 mg/kg) and CPT-11 (30 mg/kg), and found no difference in the level of SN-38 accumulation in the small intestine.[12] A significant antitumor effect of NK012 with a lower incidence of diarrhea was also dem-

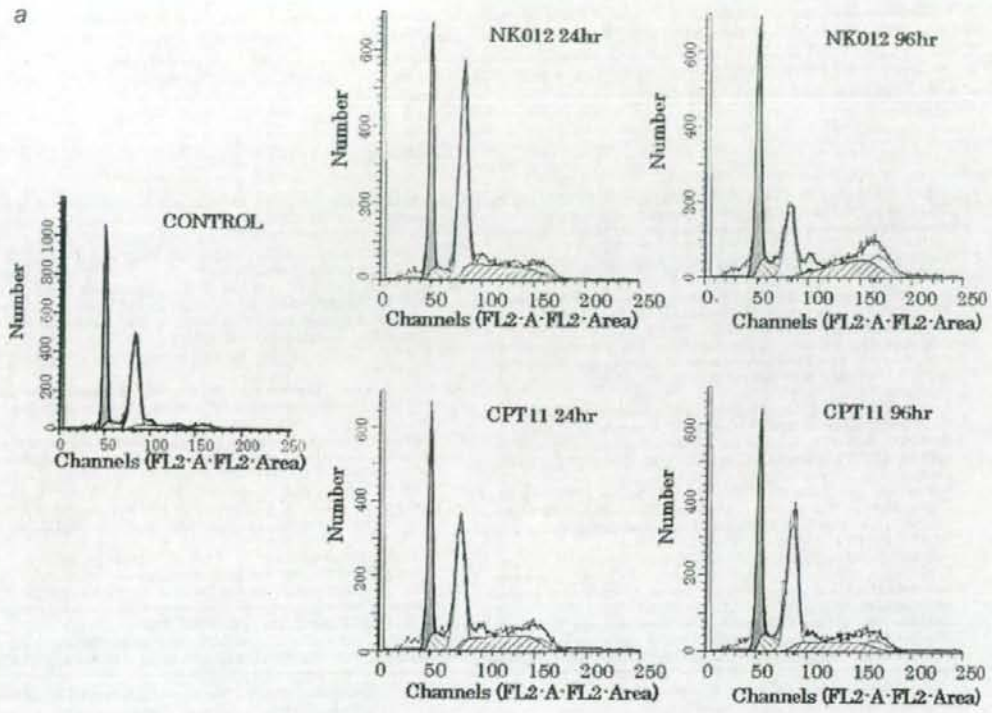

FIGURE 4 – Cell cycle analysis of HT-29 tumor cells collected 24, 48, 72 and 96 hr after administration of NK012 at 10 mg/kg alone or CPT-11 at 50 mg/kg alone using the Modfit program (Verity Software House Topsham, ME). (*a*) Cell cycle analysis of HT-29 tumor cells 24 and 96 hr after administration of NK012 at 10 mg/kg or CPT-11 at 50 mg/kg, respectively. (*b*) Cell cycle distribution of tumor cells 0, 24, 48, 72 and 96 hr after treatment with NK012 at 10 mg/kg. (*c*) Cell cycle distribution of tumor cells 0, 24, 48, 72 and 96 hr after treatment with CPT-11 at 50 mg/kg.

onstrated as compared to that observed with CPT-11 in a rat mammary tumor model.[21] Combined administration of CPT-11 with 5FU/LV infusion appears to be associated with acceptable toxicity in patients with CRC. In addition, no significant difference in the frequency of Grade 3/4 diarrhea was noted between patients treated with FOLFIRI (CPT-11 regimen with bolus and infusional 5FU/LV) and those treated with FOLFOX6 (oxaliplatin regimen with bolus and infusional 5FU/LV).[22,23] Our *in vivo* data actually revealed no severe body weight loss in the NK012/5FU group. Consequently, we expect that the NK012/5FU regimen, especially

with infusional 5FU, may be an attractive arm for a Phase III trial in CRC, with CPT-11/5FU as the control arm. We have already initiated a Phase I trial of NK012 in patients with advanced solid tumors based on the data suggesting higher efficacy and lower toxicity of this preparation than CPT-11 *in vivo*.[12]

In conclusion, we demonstrated that combined NK012 and 5FU chemotherapy exerts significantly greater antitumor activity against human CRC xenografts as compared to CPT-11/5FU, indicating the necessity of clinical evaluation of this combined regimen.

References

1. Saltz LB, Douillard JY, Pirotta N, Alakl M, Gruia G, Awad L, Elfring GL, Locker PK, Miller LL. Irinotecan plus fluorouracil/leucovorin for metastatic colorectal cancer: a new survival standard. Oncologist 2001;6:81–91.
2. Douillard JY, Cunningham D, Roth AD, Navarro M, James RD, Karasek P, Jandik P, Iveson T, Carmichael J, Alakl M, Gruia G, Awad L, et al. Irinotecan combined with fluorouracil compared with fluorouracil alone as first-line treatment for metastatic colorectal cancer: a multicentre randomised trial. Lancet 2000;355:1041–7.
3. Takimoto CH, Arbuck SG. Topoisomerase I targeting agents: the camptothecins. In: Chabner BA, Lango DL, eds. Cancer chemotherapy and biotherapy: principal and practice, 3rd ed. Philadelphia, PA: Lippincott Williams and Wilkins, 2001. 579–646.
4. Slatter JG, Schaaf LJ, Sams JP, Feenstra KL, Johnson MG, Bombardt PA, Cathcart KS, Verburg MT, Pearson LK, Compton LD, Miller LL, Baker DS, et al. Pharmacokinetics, metabolism, and excretion of irinotecan (CPT-11) following I.V. infusion of [(14)C]CPT-11 in cancer patients. Drug Metab Dispos 2000;28:423–33.
5. Rothenberg ML, Kuhn JG, Burris HA, III, Nelson J, Eckardt JR, Tristan-Morales M, Hilsenbeck SG, Weiss GR, Smith LS, Rodriguez GI, Rock MK, Von Hoff DD. Phase I and pharmacokinetic trial of weekly CPT-11. J Clin Oncol 1993;11:2194–204.
6. Guichard S, Terret C, Hennebelle I, Lochon I, Chevreau P, Fretigny E, Selves J, Chatelut E, Bugat R, Canal P. CPT-11 converting carboxylesterase and topoisomerase activities in tumour and normal colon and liver tissues. Br J Cancer 1999;80:364–70.
7. Gradishar WJ, Tjulandin S, Davidson N, Shaw H, Desai N, Bhar P, Hawkins M, O'Shaughnessy J. Phase III trial of nanoparticle albumin-bound paclitaxel compared with polyethylated castor oil-based paclitaxel in women with breast cancer. J Clin Oncol 2005;23:7794–803.
8. Muggia FM. Liposomal encapsulated anthracyclines: new therapeutic horizons. Curr Oncol Rep 2001;3:156–62.
9. Matsumura Y, Maeda H. A new concept for macromolecular therapeutics in cancer chemotherapy: mechanism of tumoritropic accumulation of proteins and the antitumor agent smancs. Cancer Res 1986;46:6387–92.
10. Zhang JA, Xuan T, Parmar M, Ma L, Ugwu S, Ali S, Ahmad I. Development and characterization of a novel liposome-based formulation of SN-38. Int J Pharm 2004;270:93–107.
11. Kraut EH, Fishman MN, LoRusso PM, Gorden MS, Rubin EH, Haas A, Fetterly GJ, Cullinan P, Dul JL, Steinberg JL. Final result of a phase I study of liposome encapsulated SN-38 (LE-SN38): safety, pharmacogenomics, pharmacokinetics, and tumor response [abstract 2017]. Proc Am Soc Clin Oncol 2005;23:139S.
12. Koizumi F, Kitagawa M, Negishi T, Onda T, Matsumoto S, Hamaguchi T, Matsumura Y. Novel SN-38-incorporating polymeric micelles, NK012, eradicate vascular endothelial growth factor-secreting bulky tumors. Cancer Res 2006;66:10048–56.
13. Chou TC, Talalay P. Quantitative analysis of dose-effect relationships: the combined effects of multiple drugs or enzyme inhibitors. Adv Enzyme Regul 1984;22:27–55.
14. Azrak RG, Cao S, Slocum HK, Toth K, Durrani FA, Yin MB, Pendyala L, Zhang W, McLeod HL, Rustum YM. Therapeutic synergy between irinotecan and 5-fluorouracil against human tumor xenografts. Clin Cancer Res 2004;10:1121–9.
15. Jain RK. Barriers to drug delivery in solid tumors. Sci Am 1994; 271:58–65.
16. Savic R, Luo L, Eisenberg A, Maysinger D. Micellar nanocontainers distribute to defined cytoplasmic organelles. Science 2003;300:615–18.
17. Kawato Y, Aonuma M, Hirota Y, Kuga H, Sato K. Intracellular roles of SN-38, a metabolite of the camptothecin derivative CPT-11, in the antitumor effect of CPT-11. Cancer Res 1991;51:4187–91.
18. Slater R, Radstone D, Matthews L, McDaid J, Majeed A. Hepatic resection for colorectal liver metastasis after downstaging with irinotecan improves survival. Proc Am Soc Clin Oncol 2003;22(abstract 1287).
19. Araki E, Ishikawa M, Iigo M, Koide T, Itabashi M, Hoshi A. Relationship between development of diarrhea and the concentration of SN-38, an active metabolite of CPT-11, in the intestine and the blood plasma of athymic mice following intraperitoneal administration of CPT-11. Jpn J Cancer Res 1993;84:697–702.
20. Atsumi R, Suzuki W, Hakusui H. Identification of the metabolites of irinotecan, a new derivative of camptothecin, in rat bile and its biliary excretion. Xenobiotica 1991;21:1159–69.
21. Onda T, Nakamura I, Seno C, Matsumoto S, Kitagawa M, Okamoto K, Nishikawa K, Suzuki M. Superior antitumor activity of NK012, 7-ethyl-10-hydroxycamptoyhecin-incorporating micellar nanoparticle, to irrinotecan. Proc Am Assoc Cancer Res 2006;47:720s(abstract 3062).
22. Tournigand C, Andre T, Achille E, Lledo G, Flesh M, Mery-Mignard D, Quinaux E, Couteau C, Buyse M, Ganem G, Landi B, Colin P, et al. FOLFIRI followed by FOLFOX6 or the reverse sequence in advanced colorectal cancer: a randomized GERCOR study. J Clin Oncol 2004;22:229–37.
23. Colucci G, Gebbia V, Paoletti G, Giuliani F, Caruso M, Gebbia N, Carteni G, Agostara B, Pezzella G, Manzione L, Borsellino N, Misino A, et al. Phase III randomized trial of FOLFIRI versus FOLFOX4 in the treatment of advanced colorectal cancer: a multicenter study of the Gruppo Oncologico Dell'Italia Meridionale. J Clin Oncol 2005; 23:4866–75.

Antitumor Effect of SN-38–Releasing Polymeric Micelles, NK012, on Spontaneous Peritoneal Metastases from Orthotopic Gastric Cancer in Mice Compared with Irinotecan

Takako Eguchi Nakajima,[1,2] Kazuyoshi Yanagihara,[3] Misato Takigahira,[3] Masahiro Yasunaga,[1] Ken Kato,[2] Tetsuya Hamaguchi,[2] Yasuhide Yamada,[2] Yasuhiro Shimada,[2] Keichiro Mihara,[3] Takahiro Ochiya,[4] and Yasuhiro Matsumura[1]

[1]Investigative Treatment Division, Research Center for Innovative Oncology, National Cancer Center Hospital East, Kashiwa, Chiba, Japan; [2]Gastrointestinal Oncology Division, National Cancer Center Hospital, [3]Central Animal Laboratory, and [4]Section for Studies on Metastasis, National Cancer Center Research Institute, Tokyo, Japan; and [5]Hematology and Oncology Department, Clinical and Experimental Oncology Division, Research Institute for Radiation Biology and Medicine, Hiroshima University, Hiroshima, Japan

Abstract

7-Ethyl-10-hydroxy-camptothecin (SN-38), an active metabolite of irinotecan hydrochloride (CPT-11), has potent antitumor activity. Moreover, we have reported the strong antitumor activity of NK012 (i.e., SN-38–releasing polymeric micelles) against human cancer xenografts compared with CPT-11. Here, we investigated the advantages of NK012 over CPT-11 treatment in mouse models of gastric cancer with peritoneal dissemination. NK012 or CPT-11 was i.v. administered thrice every 4 days at their respective maximum tolerable doses (NK012, 30 mg/kg/day; CPT-11, 67 mg/kg/day) to mice receiving orthotopic transplants of gastric cancer cell lines (44As3Luc and 58As1mLuc) transfected with the luciferase gene (n = 5). Antitumor effect was evaluated using the photon counting technique. SN-38 concentration in gastric tumors and peritoneal nodules was examined by high-performance liquid chromatography (HPLC) 1, 24, and 72 hours after each drug injection. NK012 or CPT-11 distribution in these tumors was evaluated using a fluorescence microscope on the same schedule. In both models, the antitumor activity of NK012 was superior to that of CPT-11. High concentrations of SN-38 released from NK012 were detected in gastric tumors and peritoneal nodules up to 72 hours by HPLC. Only a slight conversion from CPT-11 to SN-38 was observed from 1 to 24 hours. Fluorescence originating from NK012 was detected up to 72 hours, whereas that from CPT-11 disappeared until 24 hours. NK012 also showed antitumor activity against peritoneal nodules. Thus, NK012 showing enhanced distribution with prolonged SN-38 release may be ideal for cancer treatment because the antitumor activity of SN-38 is time dependent. [Cancer Res 2008;68(22):9318–22]

Introduction

Gastric cancer is the second most common cause of death from cancer in the world. The survival rate has remained low in patients with advanced gastric cancer, with a median survival rate of 13 months having been recently reported in a phase III trial, which has been the best outcome thus far (1). Patients with gastric cancer with scirrhous type stroma particularly showed poor prognosis even after curative resection, as well as highly progressed peritoneal dissemination (2). Because peritoneal dissemination causes several refractory symptoms such as massive ascites, intestinal obstruction, hydronephrosis, and obstructive jaundice, the quality of life of patients at the end stage of cancer is severely impaired.

Poor delivery of anticancer drugs to peritoneal metastatic cells may be one of the reasons for the poor prognosis of patients with peritoneal dissemination (3). In peritoneal nodules, the distribution and eventual diffusion of drugs to cancer cells tend to be impeded because of several obstacles such as severe fibrosis and high interstitial pressure (4, 5). On the other hand, angiogenesis was reported to be an essential factor in the development of peritoneal metastasis, and the high expression level of vascular endothelial growth factor (VEGF) in primary gastric tumors or ascitic fluid, which can enhance tumor vascular permeability, was found to be directly associated with the development of ascites and peritoneal dissemination (6–10). In addition, several factors such as kinins and nitric oxide are involved in tumor vascular permeability (11–13). Polymer-conjugated drugs and nanoparticles categorized under drug delivery system agents are favorably extravasated from the vessels into the interstitium of tumors due to the enhanced permeability and retention effect (EPR effect; refs. 14, 15). The EPR effect is based on the following pathophysiologic characteristics of solid tumor tissues: hypervascularity, incomplete vascular architecture, secretion of vascular permeability factors stimulating extravasation within cancer tissue, and absence of effective lymphatic drainage from the tumors that impedes the efficient clearance of macromolecules accumulated in solid tumor tissues. Moreover, macromolecules cannot freely leak out from normal vessels, and thus, the side effects of an anticancer agent can be reduced. Very recently, we have shown that NK012 (i.e., SN-38–releasing polymeric micelles) exerted superior antitumor activity and less toxicity than CPT-11 (15–17). In a series of studies, we showed that NK012 markedly enhanced the antitumor activity of SN-38, particularly against highly VEGF-secreting SBC-3/VEGF tumors compared with SBC-3/Neo tumors. On the other hand, it is conceivable that satisfactory drug delivery cannot be achieved in less-vascularized and highly fibrotic tumors, particularly for macromolecules. However, we observed that NK012 showed a strong antitumor activity even in the xenograft of Capan1 cells, which are pancreatic cancer cells with abundant stromal tissue, compared with CPT-11. This result suggests that NK012 can selectively accumulate in both hypervascular and hypovascular tumors with high interstitial pressure, and then induce sustained

Requests for reprints: Yasuhiro Matsumura, Investigative Treatment Division, Research Center for Innovative Oncology, National Cancer Center Hospital East, 6-5-1 Kashiwanoha, Kashiwa, Chiba 277-8577, Japan. Phone: 81-4-7134-6857; Fax: 81-4-7134-6866; E-mail: yhmatsum@east.ncc.go.jp.

doi:10.1158/0008-5472.CAN-08-2822

release of SN-38, followed by SN-38 distribution throughout the entire tumor tissues. In the present study, we evaluated the antitumor activity of NK012 against peritoneal tumor dissemination compared with that of CPT-11 using mouse models orthotopically transplanted with scirrhous gastric cancer cells, as well as against spontaneously progressing peritoneal dissemination (18, 19).

Materials and Methods

Cell cultures. 44As3 and 58As1m were previously reported as human signet-ring cell gastric cancer cell lines that spontaneously metastasize to the peritoneal cavity and produce large volumes of bloody ascites after orthotopic implantion in the gastric wall (18–21). Here, 44As3 and 58As1m cells were transfected with a complex of 4 μg of pEGF-PLuc plasmid DNA (Clontech) and 24 μL of GeneJammer reagent (Stratagene; Cloning Systems) in accordance with the manufacturer's instructions. Stable transfectants were selected in geneticin (400 μg/mL; Invitrogen), and bioluminescence was used to screen transfected clones for luciferase gene expression using the IVIS system (Xenogen). Clones expressing the luciferase gene were named 44As3Luc and 58As1mLuc. 44As3Luc and 58As1mLuc cells were maintained in RPMI 1640 supplemented with 10% FCS (Sigma), 100 IU/mL penicillin G sodium, and 100 mg/mL streptomycin sulfate (Immuno-Biological Laboratories) in a humidified atmosphere containing 5% CO_2 at 37°C.

Orthotopic models *in vivo*. Six-week-old female BALB/c *nu/nu* mice were purchased from CLEA Japan, Inc., and maintained under specific pathogen-free conditions and provided with sterile food, water, and cages. Ambient light was controlled to provide regular cycles of 12 h of light and 12 h of darkness. A total of 1×10^6 cells of 44As3Luc or 58As1Luc were inoculated into the gastric wall of each mouse after laparotomy, as described previously (18–21). *In vivo* photon counting analysis was conducted on a cryogenically cooled IVIS system using Living Image acquisition and analysis software (Xenogen). All animal procedures were performed in compliance with the Guidelines for the Care and Use of Experimental Animals established by the Committee for Animal Experimentation of the National Cancer Center; these guidelines conform to the ethical standards required by law and also comply with the guidelines for the use of experimental animals in Japan.

Drugs. NK012 was prepared by Nippon Kayaku Co., Ltd. (15). CPT-11 was purchased from Yakult Honsha Co., Ltd.

***In vivo* growth inhibition assay.** After inoculation of 44As3Luc or 58As1mLuc cells into the gastric wall (day 0), mice were randomly divided into test groups consisting of 5 mice per group. 44As3Luc mice were i.v. administered the maximum tolerated dose (MTD) of the 2 drugs via the tail vein on days 20, 24, and 28 as previously reported, that is, at 66.7 mg/kg/d for CPT-11 and 30 mg/kg/d for NK012 (15). 58As1mLuc mice were given the drugs in the same manner on days 18, 22, and 26. Photon counting analysis and body weight were measured twice a week. "Visible ascites," which was evident a few days before death in this mouse model, was used as a surrogate for survival time in consideration of animal welfare. Mice were euthanized when ascites became visible, and colonization of gastric wall by cancer cells and metastasis to the peritoneal cavity were confirmed in all the euthanized mice. Differences in relative photon counts between the treatment groups at day 42 in 44As3Luc mice and at day 81 in 58As1mLuc mice were analyzed using the unpaired *t* test.

Assay of free SN-38 in tissues. We next analyzed the biodistributions of NK012 and CPT-11 to orthotopic gastric tumors and peritoneal nodules. Twenty-six days after the inoculation of 44As3Luc cells into the gastric wall of mice, NK012 (30 mg/kg) or CPT-11 (66.7 mg/kg) was administered via the tail vein. Under anesthesia, orthotopic gastric tumor and peritoneal nodule samples were excised 1, 24, and 72 hours after injection.

Measurements of tissue concentration of free SN-38 by high-performance liquid chromatography. Samples were rinsed with physiologic saline, mixed with 0.1 mol/L glycine-HCl buffer (pH 3.0)/methanol at 5 w/w%, and then homogenized. To analyze the concentration of free SN-38, 100 μL of the tumor samples were mixed with 20 μL of 1 mmol/L phosphoric acid/methanol (1:1) and 40 μL of ultrapure water, and camptothecin (CPT) was used as the internal standard (10 ng/mL for free SN-38). The samples were vortexed vigorously for 10 s, and then filtered

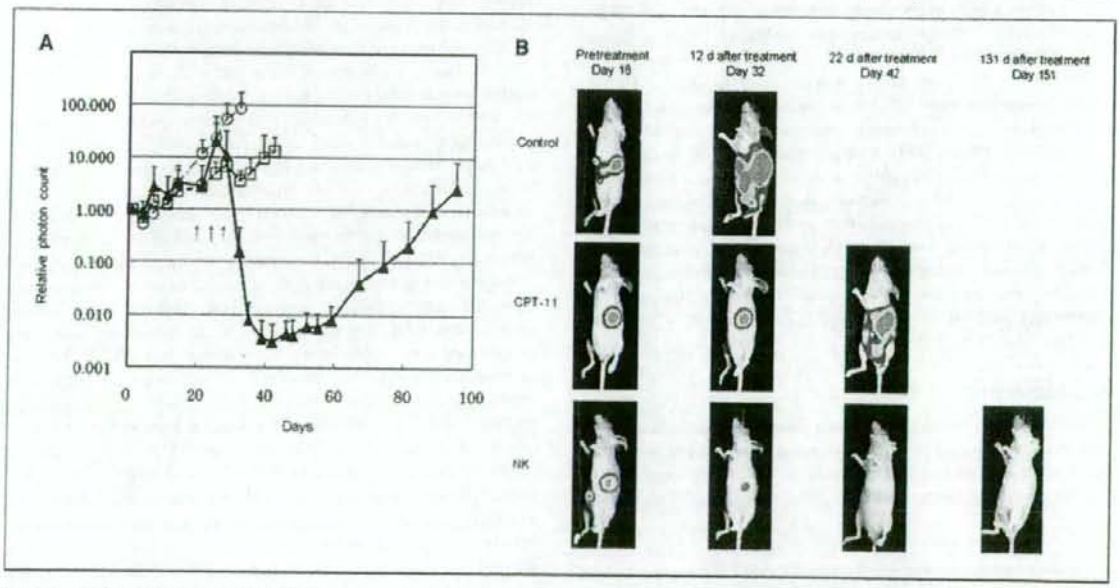

Figure 1. Effects of NK012 and CPT-11 in 44As3Luc mouse models. *A*, antitumor activity of NK012 or CPT-11 was evaluated by counting the number of photons using the IVIS system (*points*, mean; *bars*, SD; *arrows*, drug injections). Antitumor effect of each regimen on days 20, 24, and 28. (○), control; (□), CPT-11 (66.7 mg/kg/d, ×3); and (▲), NK012 (30 mg/kg/d, ×3) in 44As3Luc mouse model. *B*, images of 44As3Luc mouse model administered NK012 taken using the IVIS system on days 18, 32, 42, and 151 after inoculation of 44As3Luc cells. Data were derived from the same mice as those used in the present study.

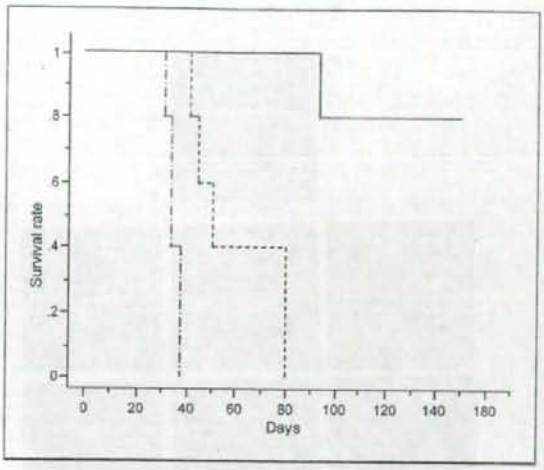

Figure 2. Survival curves of 44As3Luc mouse models. Survival curves of 44As3Luc mouse model in each regimen on days 20, 24, and 28. (–·–·–), control; (– – –), CPT-11 given at 66.7 mg/kg/d ×3; and (——), NK012 given at 30 mg/kg/d ×3.

through Ultrafree-MC Centrifugal Filter Devices with a cutoff molecular diameter of 0.45 μm (Millipore Co.). Reversed-phase high-performance liquid chromatography (HPLC) was conducted at 35°C on a Mightysil RP-18 GP column (150 × 4.6 mm; Kanto Chemical Co., Inc.). Fifty microliters of a sample were injected into an Alliance Water 2795 HPLC system (Waters) equipped with a Waters 2475 multi λ fluorescence detector. Fluorescence originating from SN-38 was detected at 540 nm with an excitation wavelength of 365 nm. The mobile phase was a mixture of 100 mmol/l ammonium acetate (pH 4.2) and methanol [11:9 (v/v)], and the flow rate was 1.0 mL/min. The content of SN-38 was calculated by measuring the relevant peak area and calibrating against the corresponding peak area derived from the CPT internal standard. Peak data were recorded using a chromatography management system (MassLynx v4.0; Waters).

Visualization of distribution of NK012 and CPT-11 by fluorescence microscopy. Mice were given fluorescein *Lycopersicon esculentum* lectin (100 μL per mouse; Vector Laboratories) to visualize tumor vasculature in the samples 5 min before anesthesia. The samples were then excised and embedded in an optimal cutting temperature compound (Sakura Finetechnochemical Co., Ltd.) and frozen at −80°C. Six-μm-thick tumor sections were then prepared using a cryostatic microtome, Tissue-Tek Cryo3 (Sakura Finetechnochemical Co., Ltd.). Frozen sections were examined under a fluorescence microscope, BIOZERO (KEYENCE), at an excitation wavelength of 377 nm and an emission wavelength 447 nm to evaluate the distribution of NK012 and CPT-11. Both drugs could be detected under the same fluorescence conditions because formulations containing SN-38 bound via ester bonds possess a particular fluorescence.

Statistical analyses. Data were expressed as mean ± SD. Data were analyzed using the Student's *t* test when groups showed equal variances (*F* test), or the Welch's test when they showed unequal variances (*F* test). *P* value of <0.05 was considered as significant. All statistical tests were two sided.

Results

Antitumor activities of NK012 and CPT-11. Comparison of the relative photon counts on day 42 in the 44As3Luc mouse model revealed significant differences in counts between mice given with NK012 and those given with CPT-11 ($P = 0.0282$; Fig. 1*A* and *B*). Similar result was obtained in the experiment with 58As gastric tumor (data not shown). The survival rates on day 150 in the 44As3Luc mouse model were 80% and 0% for the NK012 group and CPT-11 group, respectively (Fig. 2). Similar result was obtained in the experiment with 58As gastric tumor (data not shown). No marked toxic effects in terms of body weight changes were observed in any groups for any mouse models (data not shown). Only 1 mouse in the CPT-11 group of 44As1 mouse models showed diarrhea for 3 d, and any other clinical symptoms were not observed.

Tissue concentrations of free SN-38 after administration of NK012 and CPT-11. We examined the concentration-time profile of free SN-38 in orthotopic gastric tumors and peritoneal nodules in the 44As3Luc mouse model after the administration of NK012 and CPT-11 (Fig. 3*A* and *B*). Either orthotopic gastric tumors or peritoneal nodules exhibited the highest concentration of free SN-38 24 hours after NK012 administration, and 1 hour after CPT-11 administration. The highest concentrations of free SN-38 in the NK012 group were much higher than those in the CPT-11 group in either orthotopic gastric tumors or peritoneal nodules. The concentrations of free SN-38 released from NK012 in orthotopic gastric tumors were higher than those in peritoneal nodules.

Tumor tissue distribution of NK012 and CPT-11 as determined by fluorescence microscopy. Results showed that NK012 accumulation in either orthotopic gastric tumors or peritoneal nodules had been maintained from 1 hour to 72 hours after injection (Fig. 4*A*). On the other hand, CPT-11 showed maximum accumulation in either orthotopic gastric tumors or peritoneal nodules 1 hour after injection and disappeared within 24 hours (Fig. 4*B*).

Discussion

The main purpose of this study was to clarify the advantages of NK012 over CPT-11 as treatment against peritoneal metastasis spontaneously disseminated from orthotopically transplanted scirrhous gastric cancer cells in mouse models. We showed that NK012 exerted more potent antitumor activity in the mouse models used than CPT-11. Therefore, NK012 is considered promising in terms of providing clinical benefit to patients with gastric cancer showing progressing peritoneal dissemination.

CPT-11 is converted to SN-38, a biologically active and water-insoluble metabolite of CPT-11, by carboxylesterases (CE) in the liver and tumors. However, only 2% to 8% of administered CPT-11 is converted by CE in the liver and tumors to the active form SN-38 (22, 23). The conversion of CPT-11 to SN-38 also depends on genetic interindividual variability of the activity of CE (24). Thus, the direct use of SN-38 might be of great advantage and is attractive for cancer treatment. We have recently shown that NK012 (i.e., SN-38–releasing polymeric micelles) exerted superior antitumor activity and less toxicity than CPT-11 (15–17). The mean particle size of NK012 is 20 nm in diameter. NK012 can release SN-38 under neutral conditions even in the absence of CE because SN-38, which is bound to the blockcopolymer by phenolic ester binding, is stable under acidic conditions but relatively labile under neutral and mild alkaline conditions. The release rate of SN-38 from NK012 under physiologic conditions is quite high, that is, >70% of SN-38 is gradually released within 48 hours.

In this study, we used mouse models with orthotopically transplanted human scirrhous gastric cancer cells showing spontaneously progressing peritoneal dissemination, which we

reported previously (18, 19, 21). These models can imitate more realistically the progressing mode of human peritoneal dissemination of gastric cancer than conventional experimental models directly transplanted with cancer cells i.p. Moreover, our models enabled us to quantitatively evaluate drug antitumor effect even against peritoneal dissemination without having to sacrifice the animal and perform autopsy through the use of gastric cancer cells transfected with the luciferase gene and by applying photon counting analysis, having already verified the significant correlation between tumor volume and photon counts in a previous report (19).

For *in vivo* growth inhibition assay, drug administration was started on day 18 or 20 after cell inoculation into the gastric wall, when small peritoneal metastatic nodules and a small degree of ascites had appeared. The present results showed that NK012 had more potent antitumor activity than CPT-11 in the mouse models tested, suggesting its effectiveness against peritoneal dissemination of gastric cancer in the clinical setting.

In the pharmacologic evaluation, we could confirm the more enhanced distribution of NK012 than CPT-11 to not only orthotopic gastric tumors but also peritoneal nodules by quantifying SN-38 concentration in the tumors and visualization of fluorescence originating from NK012 or CPT-11 distributed in the tumors. Because CPT-11 or SN-38 has been reported to possess time-dependent growth-inhibitory activity against tumor cells, this prolonged retention of NK012 in the tumors and the sustained release of free SN-38 from NK012 may be responsible for its more potent antitumor activity observed in the present study (25). On the other hand, CPT-11 disappeared from the tumors before exerting sufficient antitumor activity. For both drugs, however, the concentrations of SN-38 in orthotopic gastric tumors were higher than those

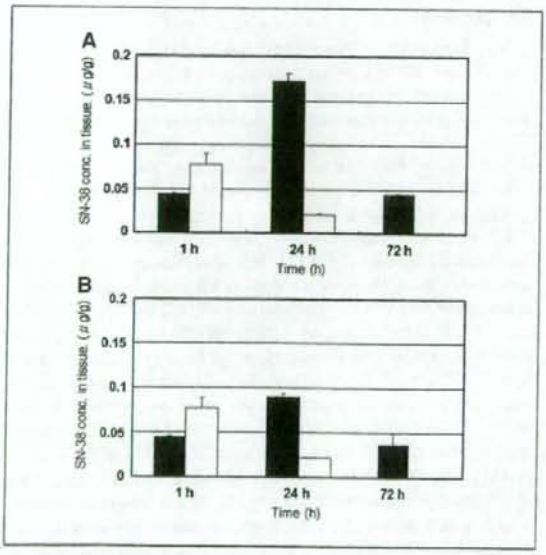

Figure 3. Concentration-time profile of free SN-38. NK012 (30 mg/kg) or CPT-11 (66.7 mg/kg) was injected 26 d after implantation of 44As3Luc gastric cancer cells (*columns*, mean; *bars*, SD). *A*, concentration (*conc.*) of free SN-38 in orthotopic gastric tumor tissue of 44As3Luc mouse model after administration of NK012 (*black column*) and CPT-11 (*white column*). *B*, concentration of free SN-38 in peritoneal nodules of 44As3Luc mouse model after administration of NK012 (*black column*) and CPT-11 (*white column*).

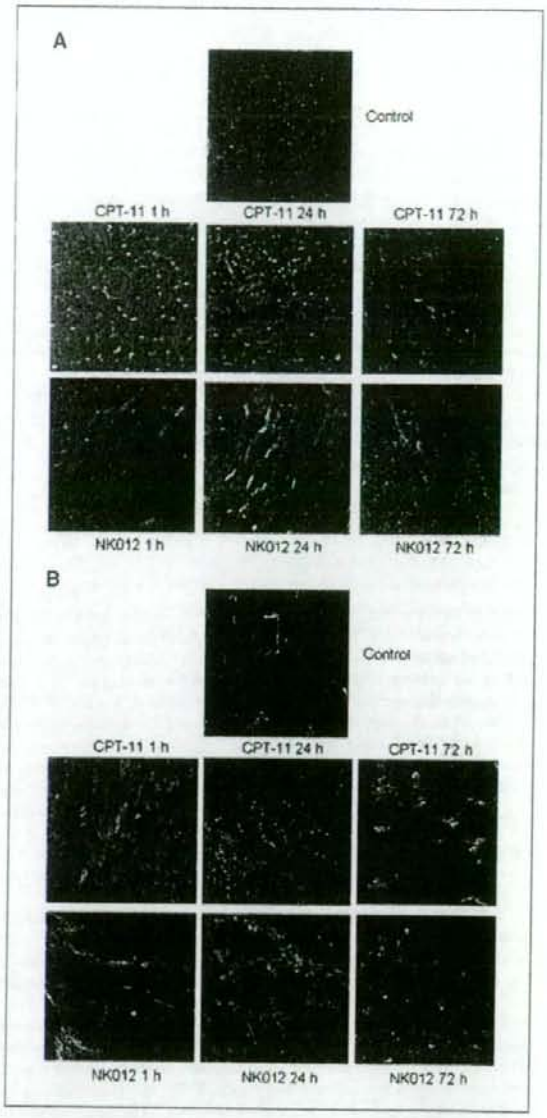

Figure 4. Tissue distribution of NK012 and CPT-11 as determined by fluorescence microscopy. Orthotopic gastric tumors or peritoneal nodules of 44As3Luc mouse model were excised 1, 24, and 72 h after i.v. injection of NK012 (30 mg/kg) or CPT-11 (66.7 mg/kg). Each mouse was i.v. administered with fluorescein-labeled *Lycopersicon esculentum* lectin just before being sacrificed to detect tumor blood vessels. Frozen sections were examined under a fluorescence microscope at an excitation wavelength of 377 nm and an emission wavelength of 447 nm. The same fluorescence condition can be applied for visualizing NK012 and CPT-11 fluorescence. Free SN-38 cannot be detected under this fluorescence condition. *A*, distribution of NK012 or CPT-11 in orthotopic gastric tumors (×100). *B*, distribution of NK012 or CPT-11 in peritoneal nodules (×100).

in peritoneal nodules. This is consistent with previous reports stating the poor delivery of anticancer drugs to peritoneal metastatic cells probably because of some obstacles such as abundant interstitium or high interstitial pressure. To date, we reported that NK012 can

more selectively accumulate and retain longer in various tumor xenografts transplanted s.c. compared with CPT-11 (15–17). In the present study, we succeeded in demonstrating higher accumulation and longer retention of NK012 compared with CPT-11 in orthotopic and peritoneal disseminated gastric cancer model that is closer to human gastric cancer in clinics.

Peritoneal dissemination sometimes causes intestinal obstruction, which enhances the enterohepatic circulation of SN-38 after direct damage to the small intestine, and makes the use of CPT-11 difficult (26, 27). In the present study, no mouse in the NK012 group developed diarrhea. The dose-limiting toxic effects of CPT-11 seem to be neutropenia and diarrhea. In our previous data, however, there was no significant difference in the level of SN-38 in the small intestine between mice treated with NK012 and mice treated with CPT-11 despite the higher plasma area under the concentration of NK012 than CPT-11 (15). Moreover, no serious diarrhea has been reported even at the MTD dose in two phase I clinical trials against advanced solid tumors in Japan and the US (28, 29).

In conclusion, we showed that NK012 exerts significantly more potent antitumor activity against peritoneal dissemination of scirrhous gastric cancer cells than CPT-11, indicating the possibility of the clinical evaluation of this drug in patients with disseminated grastic cancer.

Disclosure of Potential Conflicts of Interest

No potential conflicts of interest were disclosed.

Acknowledgments

Received 7/23/2008; revised 9/2/2008; accepted 9/16/2008.

Grant support: Third Term Comprehensive Contorol Research for Cancer from the Ministry of Health, Labor and Welfare of Japan (Y. Matsumura) and a Grant-in-Aid for Scientific Research on Priority Areas from the Ministry of Education, Culture, Sports, Science and Technology (Y. Matsumura).

The costs of publication of this article were defrayed in part by the payment of page charges. This article must therefore be hereby marked *advertisement* in accordance with 18 U.S.C. Section 1734 solely to indicate this fact.

References

1. Koizumi W, Narahara H, Hara T, et al. S-1 plus cisplatin versus S-1 alone for first-line treatment of advanced gastric cancer (SPIRITS trial): a phase III trial. Lancet Oncol 2008;9:215–21.
2. Maehara Y, Moriguchi S, Orita H, et al. Lower survival rate for patients with carcinoma of the stomach of Borrmann type IV after gastric resection. Surg Gynecol Obstet 1992;175:13–6.
3. Yonemura Y. Mechanisms of drug resistance in gastric cancer. In: Yonemura Y, editor. Contemporary Approaches Toward Cure of Gastric Cancer. Kanazawa: Maeda Shoten Co. Ltd.; 1996. p. 87–91.
4. Yashiro M, Chung YS, Nishimura S, Inoue T, Sowa M. Fibrosis in the peritoneum induced by scirrhous gastric cancer cells may act as "soil" for peritoneal dissemination. Cancer 1996;77:1668–75.
5. Jain RK. Barriers to drug delivery in solid tumors. Sci Am 1994;271:58–65.
6. Senger DR, Galli SJ, Dvorak AM, Perruzzi CA, Harvey VS, Dvorak HF. Tumor cells secrete a vascular permeability factor that promotes accumulation of ascites fluid. Science 1983;219:983–5.
7. Dvorak HF, Brown LF, Detmar M, Dvorak AM. Vascular permeability factor/vascular endothelial growth factor, microvascular hyperpermeability, and angiogenesis. Am J Pathol 1995;146:1029–39.
8. Nagy JA, Masse EM, Herzberg KT, et al. Pathogenesis of ascites tumor growth: vascular permeability factor, vascular hyperpermeability, and ascites fluid accumulation. Cancer Res 1995;55:360–8.
9. Boocock CA, Charnock-Jones DS, Sharkey AM, et al. Expression of vascular endothelial growth factor and its receptors flt and KDR in ovarian carcinoma. J Natl Cancer Inst 1995;87:506–16.
10. Aoyagi K, Kouhuji K, Yano S, et al. VEGF significance in peritoneal recurrence from gastric cancer. Gastric Cancer 2005;8:155–63.
11. Maeda H, Matsumura Y, Kato H. Purification and identification of [hydroxyprolyl3]bradykinin in ascitic fluid from a patient with gastric cancer. J Biol Chem 1988;263:16051–4.
12. Matusmura Y, Maruo K, Kimura M, Yamamoto T, Konno T, Maeda H. Kinin-generating cascade in advanced cancer patients and *in vitro* study. Jpn J Cancer Res 1991;82:732–41.
13. Wu J, Akaike T, Hayashida K, et al. Identification of bradykinin receptors in clinical cancer specimens and murine tumor tissues. Int J Cancer 2002;98:29–35.
14. Matsumura Y, Maeda H. A new concept for macromolecular therapeutics in cancer chemotherapy: mechanism of tumoritropic accumulation of proteins and the antitumor agent smancs. Cancer Res 1986;46:6387–92.
15. Koizumi F, Kitagawa M, Negishi T, et al. Novel SN-38-incorporating polymeric micelles, NK012, eradicate vascular endothelial growth factor-secreting bulky tumors. Cancer Res 2006;66:10048–56.
16. Nakajima TE, Yasunaga M, Kano Y, et al. Synergistic antitumor activity of the novel SN-38-incorporating polymeric micelles, NK012, combined with 5-fluorouracil in a mouse model of colorectal cancer, as compared with that of irinotecan plus 5-fluorouracil. Int J Cancer 2008;122:2148–53.
17. Saito Y, Yasunaga M, Kuroda J, Koga Y, Matsumura Y. Enhanced distribution of NK012, a polymeric micelle-encapsulated SN-38, and sustained release of SN-38 within tumors can beat a hypovascular tumor. Cancer Sci 2008;99:1258–64.
18. Yanagihara K, Takigahira M, Tanaka H, et al. Development and biological analysis of peritoneal metastasis mouse models for human scirrhous stomach cancer. Cancer Sci 2005;96:323–32.
19. Yanagihara K, Takigahira M, Takeshita F, et al. A photon counting technique for quantitatively evaluating progression of peritoneal tumor dissemination. Cancer Res 2006;66:7532–9.
20. Yanagihara K, Tanaka H, Takigahira M, et al. Establishment of two cell lines from human gastric scirrhous carcinoma that possess the potential to metastasize spontaneously in nude mice. Cancer Sci 2004;95:575–82.
21. Arao T, Yanagihara K, Takigahira M, et al. ZD6474 inhibits tumor growth and intraperitoneal dissemination in a highly metastatic orthotopic gastric cancer model. Int J Cancer 2006;118:483–9.
22. Slatter JG, Schaaf LJ, Sams JP, et al. Pharmacokinetics, metabolism, and excretion of irinotecan (CPT-11) following I.V. infusion of [(14)C]CPT-11 in cancer patients. Drug Metab Dispos 2000;28:423–33.
23. Rothenberg ML, Kuhn JG, Burris HA III, et al. Phase I and pharmacokinetic trial of weekly CPT-11. J Clin Oncol 1993;11:2194–204.
24. Guichard S, Terret C, Hennebelle I, et al. CPT-11 converting carboxylesterase and topoisomerase activities in tumour and normal colon and liver tissues. Br J Cancer 1999;80:364–70.
25. Kawato Y, Aonuma M, Hirota Y, Kuga H, Sato K. Intracellular roles of SN-38, a metabolite of the camptothecin derivative CPT-11, in the antitumor effect of CPT-11. Cancer Res 1991;51:4187–91.
26. Araki E, Ishikawa M, Iigo M, Koide T, Itabashi M, Hoshi A. Relationship between development of diarrhea and the concentration of SN-38, an active metabolite of CPT-11, in the intestine and the blood plasma of athymic mice following intraperitoneal administration of CPT-11. Jpn J Cancer Res 1993;84:697–702.
27. Atsumi R, Suzuki W, Hakusui H. Identification of the metabolites of irinotecan, a new derivative of camptothecin, in rat bile and its biliary excretion. Xenobiotica 1991;21:1159–69.
28. Kato K, Hamaguchi T, Shirao K, et al. Interim analysis of phase I study of NK012, polymer micelle SN-38, in patients with advanced cancer. Proc Am Soc Clin Oncol GI 2008 (Abs #485).
29. Burris HA III, Infante JR, Spigel DR, et al. A phase I dose-escalation study of NK012. Proc Am Soc Clin Oncol 2008 (Abs #2358).

SN-38内包高分子ミセルNK012

日米独立 phase Ⅰ試験

特集　臨床開発中のDDS製剤

堀田洋介・濱口哲弥[*1]，土井俊彦[*2]，高梨正哉[*3]

Two independent phase I trials of NK012, SN-38 incorporating micellar nanoparticle for patients with advanced cancer, opened in Japan and United States of America

NK012 is a micellar drug that incorporates the CPT-11 active metabolite SN-38. Currently, CPT-11 is used for the treatment of a wide variety of cancer ; however, it is expected that NK012 may show stronger antitumor effects of SN-38 than CPT-11. A phase I trial of NK012 was performed separately in the US and Japan, and the result of each trial showed that NK012 is well tolerated, suggesting its clinical usefulness.

It is anticipated that the subsequent phase Ⅱ and Ⅲ trials will demonstrate the advantages of NK012 as a drug delivery system.

NK012は，CPT-11の活性体のSN-38を内包した高分子ミセル化製剤である．現在CPT-11は，幅広いがん腫に用いられているが，NK012はそのCPT-11と比較しSN-38の薬効を効率よく発現できると考えられている．日本とアメリカでそれぞれ独立したNK012の臨床第Ⅰ相試験が行われ，その結果が報告された．

これらの結果から，NK012の忍容性が確認され有用性が示唆された．次相からの試験において，そのDDS製剤としての特徴をはっきり証明することが期待されている．

Yousuke Horita・Tetsuya Hamaguchi[*1]*, Toshihiko Doi*[*2]*, Masaya Takanashi*[*3]

key words : NK012, micellar nanoparticle

固形腫瘍に対する抗がん剤治療におけるDDS製剤の役割は，より選択的に薬剤をがん罹患部に到達させることで治療効果を高め，かつ同時に抗がん剤に伴う有害反応の軽減を図ることにある．その理論的背景となるのが，EPR(enhanced permeability and retention)効果である．固形腫瘍においては，一般的に新生腫瘍血管が増生している一方で，それに見合うリンパ回収系の増生がなく，腫瘍局所においては著しい血管透過性の亢進が起きていることによって，正常血管では血管外に漏出しにくい高分子物質も腫瘍血管からは漏出しやすく，かつ，腫瘍局所でいったん漏出した高分子物質はその場に停滞しやすいといった理論をEPR効果とよぶ[1~3]．このEPR効果を利用して，リポソーム製剤やミセル製剤が開発され，いくつもの臨床試験が行われ，一部は臨床実用化されている．

今回，SN-38内包の高分子ミセル化製剤であるNK012の第Ⅰ相試験が日本とアメリカで独立して行われ，その結果が報告されたので，その内容を概説したい．

NK012の概要

NK012は，イリノテカン(CPT-11)の活性体のSN-38を内包した高分子ミセル化製剤である．難溶性であるSN-38をポリエチレングリコールとポリグルタミン酸のブロックコポリマーに化学的に結合させると，外核に親水性鎖，内核に疎水性鎖を有するナノパーティクルを形成する(図1)．もともとSN-38は，植物アルカロイドであるcamptothecinから，その腫瘍効果を高め，毒性を軽減した化合物として合成された[4]．しかしながら，SN-38が水難溶性であったため，SN-38の誘導体であるCPT-11が開発され，実臨床に展開され，現在，大腸がん，

[*1] Gastrointestinal Oncology Division, National Cancer Center Hospital　国立がんセンター中央病院消化器内科
[*2] Department of Gastrointestinal Medicine, National Cancer Center Hospital, East　国立がんセンター東病院消化管内科
[*3] Nippon Kayaku Co., Ltd.　日本化薬株式会社

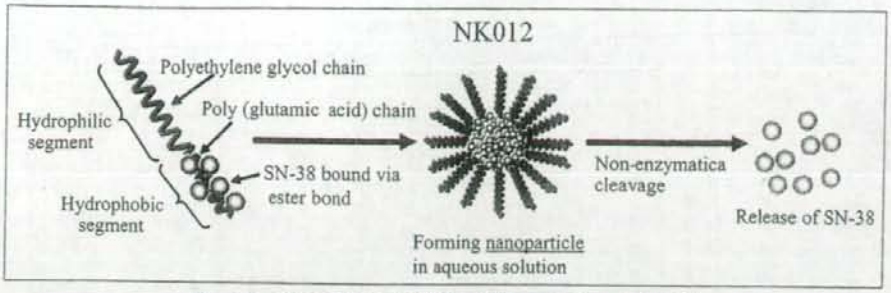

図1 NK012(SN-38内包ミセル体)の構造 (Doi T et al., 2008)[10]

肺がん，卵巣がんなど幅広いがん腫において用いられている．

CPT-11の抗腫瘍活性は，体内でcarboxylesterase(CE)によりSN-38に変換され効果を発揮すると考えられているが，その変換効率が10%以下であること[5,6]とCE活性には個人差があること[7]が知られており，より効率的で有効な抗腫瘍効果を得るためには，SN-38を直接利用することが有用であると考えられていた．そこで，水難溶性のSN-38をミセル化することで，静脈内投与を可能としたのがNK012である．

NK012の平均粒径は約20 nmであり，リポソーム製剤や他のミセル体抗がん剤と比較するとやや小さめである．37℃のPBS(phosphate buffered saline)内でのNK012からSN38のリリース速度は，24時間で57%，48時間で74%である一方，37℃の5%ブドウ糖液下でのリリースは，24時間で1%，48時間で3%と低値を示しており，このことからもNK012は投与前の環境では安定であり，かつ投与後，生体内では比較的速やかにSN38をリリースする性質が示された[8]．

各種細胞株における*in vitro*での細胞増殖抑制効果(IC_{50})は，CPT-11の約43～340倍と強い抗腫瘍効果を示し[8]，また，ヌードマウスの皮下に移植したヒト腫瘍6系(結腸がん3系，胃がん2系，小細胞がん1系)に対する抗腫瘍効果試験においても，NK012は検討したすべてのヒト腫瘍系に対してCPT-11に比較し高い有効性を示した[9]．ここでのCPT-11と同等の効果を示すNK012の投与量はSN-38換算量としてCPT-11の1/5～1/10であり，NK012はミセル形成型高分子プロドラッグにすることによってSN-38の薬効を効率よく発現できることが示唆された．

投与量 (mg/m²)	症例数	
2	1	AT法による100%増量
4	1	
8	1	増量幅をFibonacci変法に切替え
12	3	
16	3	
20	3	増量幅を4mg/m²増に変更
24	3	
28	3	DLT 1/3 → 3例追加
28	3	DLT 2/6(1例確定できず) → 3例追加
28	3	
計	24	(Doi T et al., 2008)[10]

図2 増量経過および症例数
AT法：accelerated titration method

本剤の毒性については，前臨床試験においてリンパ・造血器，消化管，生殖器，および皮膚への殺細胞作用に基づく毒性が認められた．DDS製剤に期待される効果の一つとして，正常組織への分布の減少による有害事象の軽減がある．

CPT-11の用量制限毒性の一つである下痢は，CPT-11とSN-38の腸管への直接障害が原因の一つと考えられている．NK012とCPT-11投与後の小腸におけるfree SN-38の濃度分布の検討では，両者に差は認められなかった[8]．しかし，NK012はCPT-11自体としての腸管障害がないぶん，下痢症状を減弱させる可能性が示唆され，恩田らは，ラットのモデルを用いてNK012がCPT-11に比較し強い抗腫瘍効果を発揮すると同時に，下痢症状を軽減させると報告している[9]．

表1 血液毒性

Dose (mg/m²)	n	白血球減少				好中球減少				血小板減少			
		Grade				Grade				Grade			
		1	2	3	4	1	2	3	4	1	2	3	4
2~8	3	0	0	0	0	0	0	0	0	0	0	0	0
12	3	0	1	1	0	1	0	1	0	1	0	1	0
16	3	1	2	0	0	2	0	1	0	1	0	0	0
20	3	1	0	2	0	1	0	0	2	0	1	0	0
24	3	0	2	1	0	0	0	2	1	3	0	0	0
28	9	0	1	5	3	0	0	4	5	3	3	0	0
Total	24	2	6	9	3	4	0	8	8	8	4	1	0

(Doi T et al., 2008)[10]

表2 非血液毒性

	2~20 mg/m² (n=12)				24 mg/m² (n=3)				28 mg/m² (n=9)			
	Grade				Grade				Grade			
	1	2	3	4	1	2	3	4	1	2	3	4
悪心	8	2	0	0	3	0	0	0	3	3	1	0
食欲不振	6	3	0	0	3	0	0	0	3	2	2	0
嘔吐	3	1	0	0	0	0	0	0	2	3	0	0
下痢	3	0	0	0	0	1	0	0	4	4	0	0
疲労	7	0	0	0	2	1	0	0	4	2	0	0
発熱性好中球減少	0	0	0	0	0	0	0	0	0	0	1	0
感染	0	1	0	0	0	0	0	0	0	0	1	0
心房粗動	0	0	0	0	0	0	0	0	0	0	1	0
脱毛	7	1	-	-	1	2	-	-	5	3	-	-
γGTP増加	0	1	1	0	1	0	0	0	2	1	0	0

(Doi T et al., 2008)[10]

NK012第I相試験：日本

筆者らは，2008年10月21~24日までスイスのジュネーヴで開催されたEORTC-NCI-AACRにおいて，日本におけるNK012第I相試験の報告を行った[11]．その報告の概要を以下にあげていく．

1. 試験の目的

NK012の用量制限毒性(DLT)，最大耐量(MTD)，有害事象などを評価項目とした安全性や薬物動態(PK)の検討を行い，第II相試験での推奨用量(RD)を決定することであり，また可能な症例で抗腫瘍効果を確認することであった．

2. 方　法

対象は，組織学的に悪性腫瘍と診断され，標準治療に無効もしくは適切な治療がない症例で，主要臓器機能が充分保持され，PS(performance status)が0-2，20歳以上74歳未満などの条件にて選択した．

開始投与量は，前臨床試験においてマウスLD_{10}の1/10が17.3 mg/m²，イヌのTDL(toxic dose low)の1/3が2.13 mg/m²であったことから，2 mg/m²と設定し，規定に沿って投与量を増量していった(図2)．用法・用量は5%ブドウ糖液250 mLに溶解し，30分で点滴静注を行い，これを3週間ごとに実施した．毒性の評価はCTCAE(Ver.3.0)で行い，抗腫瘍効果の判定はRECISTを用いて行った．

また，血液・尿をサンプルとし，PK解析も実施した．DLTの規準は，①5日以上継続するgrade 4の好中球減少(<500/μL)，②grade 4の血小板減少(<25,000/μL)，③grade 3以上の非血液毒性(grade 3までの食欲不振，悪心，嘔吐，過敏症は除く)とした．

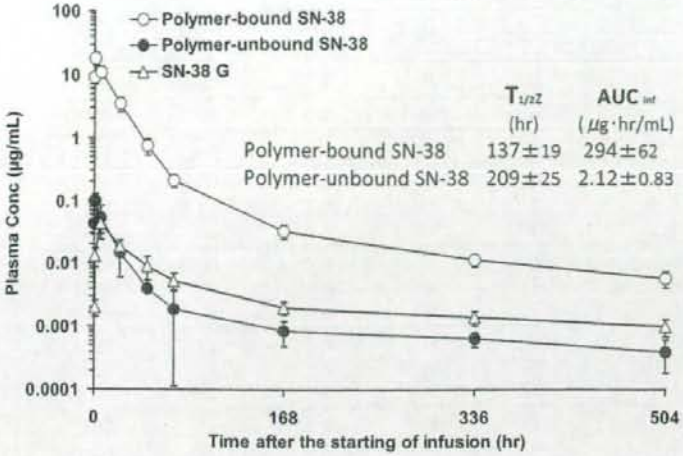

図3
NK012(28 mg/m²)投与後の
各PKパラメーター血中濃度
(n=9)

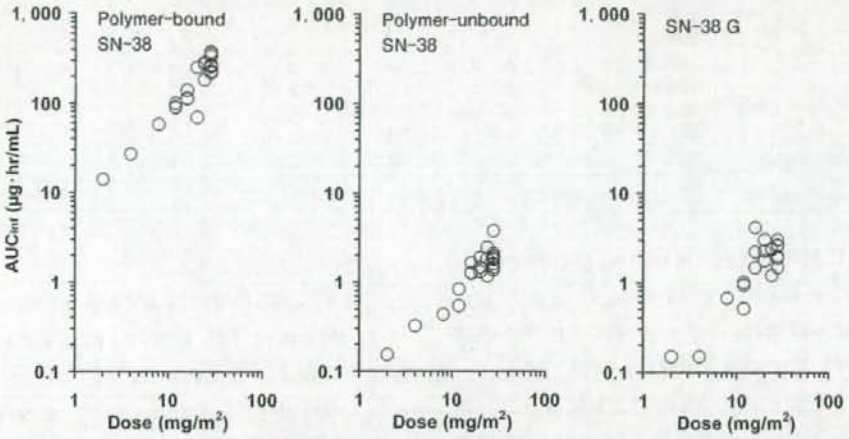

図4 投与量とAUCの関係 (Doi T et al. 2008)[10]

3. 結 果

症例の内訳は全24例中，大腸がんが最多で12例，ついで膵臓がん4例，小細胞肺がん3例，食道がん3例，非小細胞肺がん1例，肺カルチノイド1例であった．増量法は，開始用量を2 mg/m² としaccelerated titration methodにて1例ごとに100%増量した．8mg/m² 投与群において，好中球数が投与前値にくらべて約50%減少したため，効果安全性評価委員会に諮り，安全性を考慮し，以降はFibonacci変法に変更し，増量した．その後，20mg/m² 投与群において，grade4の好中球減少が出現したため，増量幅を以降4mg/m² に変更した．28 mg/m² 投与群において，DLTであるgrade3の発熱性好中球減少が出現したため，3例追加検討した．その追加3例中1例にgrade4の好中球減少が発現したが，その時点ではDLTの評価が困難であったため，効果安全性評価委員会の答申を受け，さらに3例再追加し，28 mg/m² 投与群は計9例での評価となった．

また，UGT1A1*28/*28のホモ接合体を持つ症例に対する増量も計画されていたが，該当する症例はいなかった．

有害事象に関してDLTは，16 mg/m² 投与群に1例，24 mg/m² 投与群に1例，28 mg/m² 投与群に5

表3　NK012の効果

投与量 (mg/m^2)	原疾患	年齢	性別	前治療 CPT-11	投与コース	効果
2	大腸がん	74	M	あり	2	PD
4	大腸がん	69	M	あり	1	PD
8	膵臓がん	65	M	なし	2	PD
12	膵臓がん	55	M	なし	4	SD
	大腸がん	71	M	あり	10	SD
	大腸がん	41	F	あり	2	PD
16	大腸がん	60	F	あり	4	SD
	大腸がん	61	M	あり	6	SD
	大腸がん	63	M	あり	2	PD
20	大腸がん	59	M	あり	6	SD
	小細胞肺がん	66	M	あり	7	SD
	大腸がん	49	M	あり	2	PD
24	小細胞肺がん	70	M	あり	10	(SD)
	膵臓がん	60	M	なし	3	PD
	非小細胞肺がん	68	F	なし	4	SD
28	小細胞肺がん	62	F	あり	1	NE
	大腸がん	67	M	あり	10	SD
	大腸がん	66	M	あり	3	PD
	膵臓がん	58	F	なし	2	PD
	食道がん	57	M	なし	7	PR
	大腸がん	56	F	あり	2	PD
	食道がん	51	M	なし	2	PD
	肺カルチノイド	45	M	なし	7+	PR
	食道がん	73	M	なし	4	SD

例の計7例に認められた．16 mg/m^2 投与群では，4コース目にgrade 3のγGTP増加が認められ，24 mg/m^2 投与群では，3コース目に5日以上継続するgrade 4の好中球減少が認められた．28 mg/m^2 投与群では，1コース目の9例中2例に5日以上継続するgrade 4の好中球減少およびgrade 3の発熱性好中球減少がそれぞれ1例ずつ認められ，2コース目以降に5日以上継続するgrade 4の好中球減少，好中球減少を伴う感染(grade 3)，およびgrade 3の心房粗動をそれぞれ1例ずつ認められた．

増量規定では，28 mg/m^2 投与群9例中1コース目のDLT発現が2例であったことから，さらなる増量は可能であったが，2コース目以降に発現したDLTなども含め，効果安全性評価委員会で検討した結果，本試験ではこれ以上の増量は行わないこととし，MTDを28 mg/m^2 と判断し，また，主なDLTがG-CSFなどでコントロール可能な好中球減少であったことから，推奨投与量を28 mg/m^2 とした．

つぎに，副作用発現状況を**表1**に示す．血液毒性は，20 mg/m^2 投与群では2例grade 4の好中球減少が出現し，28 mg/m^2 投与群では全例がgrade 3以上の好中球減少を認めていた．血小板減少は，28 mg/m^2 投与群ではgrade 2が3例であった．非血液毒性については，主な事象は消化管毒性であったが，多くは一過性で，問題となると考えられた下痢については，28 mg/m^2 投与群ではgrade 3以上はなく，grade 2が4例であった(**表2**)．

PK結果を**図3**に示す．これは28 mg/m^2 投与群におけるPK結果で，ポリマー結合SN-38，非結合SN-38，SN-38Gともに長時間にわたって血中濃度を保っていることがわかる．既報告[11]のCPT-11のPKと比較し，$T_{1/2}$ではポリマー非結合SN-38はSN-38の15倍，ポリマー結合SN-38はCPT-11の30倍，AUCはそれぞれ2倍，10倍と，$T_{1/2}$・AUCともに高値を示しており，NK012の血中滞留性の高さが確認された．**図4**は投与量とAUCについて